



Jorge Emídio Costa dos Santos
Licenciado em Ciências de Engenharia em Micro e
Nanotecnologias

Immobilization of Therapeutic Deep Eutectic Solvents within fibers for drug delivery applications

Dissertação para obtenção do Grau de Mestre em
Engenharia de Micro e Nanotecnologias

Orientador: Dr. Alexandre Babo de Almeida Paiva, Investigador
Auxiliar, Departamento de Química, FCT NOVA.

Coorientador: Dr. João Paulo Miranda Ribeiro Borges, Prof.
Associado com Agregação Departamento de Ciências dos
Materiais, FCT NOVA.



Outubro, 2018

*“The mind that opens to a new
idea never returns to its
original size.”*

Albert Einstein

Acknowledgements

À minha família, minha mãe, meu pai, avós e irmão um enorme obrigado por todo o apoio e carinho ao longo destes anos. Sei que não foi fácil quando me deixaram aqui tão longe de casa e não tem sido fácil gerir a distância, mas obrigado por me terem apoiado nas minhas ambições e por estarem sempre lá quando preciso. Amo-vos imenso.

A todos os meus professores, ao professor Geraldês um grande abraço de gratidão por todo o conhecimento que me transmitiu e especialmente pela amizade que ficou. À professora Dulce e à Manuela Rainho não há palavras que traduzam a gratidão que tenho para convosco, serão exemplos que levarei para a vida inteira. À Joana Pinto, à Ana Batista, professor Lavareda, professora Godinho, professora Susete, professor Pedro Batista um grande abraço e obrigado por tudo o que me ensinaram e por todo o apoio prestado.

Aos meus orientadores, professor João Paulo Borges obrigado por todo o apoio e acompanhamento num dos maiores desafios que enfrentei até hoje. Obrigado por me ter disponibilizado o laboratório de biomateriais e o seu material e obrigado pela sua disponibilidade e entrega sempre que necessitei. Foi um privilégio trabalhar consigo e sem dúvida que gostaria de o voltar a fazer. Ao Alexandre que, apesar de sermos um pouco de mundos opostos, sempre se esforçou para me por à vontade com aquilo que eu não conhecia ou não compreendia muito bem, foi muito bom ter-te conhecido e ter trabalhado contigo, um muito obrigado.

E por fim, a todos os meus amigos, que tornarão esta etapa a mais importante da minha vida até hoje. Ao Miguel Furtado, grande Miguel, obrigado pelas inúmeras discussões à volta do conteúdo das disciplinas e dos trabalhos, pelas explicações matemáticas e pela imensa camaradagem ao longo destes 5 anos. Ao Bolacha, à Sílvia, à Sofia Pádua, à Mariana, ao Duarte, à Bea, à Íris, ao Guilherme, ao Carapinha... epah, sem vocês o que era a FCT? À Kate, ao Ricardinho, à Raquel, ao André, à Inês, à Helena, ao Gabriel, à Mónica, ao Bubbles, não importa onde esteja, faça sol ou faça chuva, vocês são todos para a vida e mais não é preciso dizer, fizeram destes 5 anos uma aventura memorável e fantástica. Um grande obrigado a todos.

Por último, mas não menos importante, um grande abraço a ti Catarina pela paz que me trazes, apoio e carinho que me dás. Desde que apareceste que fazes a diferença na tua forma única de me motivar a trabalhar quando não quero e ajudar quando estou triste. Obrigado por tudo o que és. E obrigado a Deus por ter posto todas estas pessoas maravilhosas na minha vida com as quais tive a oportunidade de crescer e de me tornar numa versão melhor de mim próprio. Grato do fundo do coração.

Abstract

The search for effective drug delivery systems has been subject of research over the last decades. Due the body's many physiological barriers and the urgent need for increased bioavailability of active pharmaceutical ingredients (APIs), the efficient administration and therapeutic effect of a drug has become a great and important challenge nowadays. Transdermal drug delivery has recently gained attention in this field being mostly limited by the though barrier of the *stratum corneum*. Many studies have been conducted in order to enhance skin permeation of a drug and many transdermal patches are now available for commercial use due to its commodity and non-evasive properties. In this work, a therapeutic eutectic system designed to be effective at delivering ibuprofen through the skin was incorporated into a polymeric fibrous membrane produced by the Solution Blow Spinning method. An optimization of the fibrous membranes production was made, the impact of the Solution Blow Spinning parameters in fiber diameter was studied, retention capacity of the drug was evaluated as well as UV crosslinking efficiency and mechanical strength of the obtained membranes. The Solution Blow Spinning method showed to be simple and efficient at producing micrometric fibers with mean diameters ranging from 1 to 5 μm . The obtained membranes showed to be capable of retaining the eutectic drug but they were quite fragile and an overtime-controlled release was not achieved due to the polymer high solubility in water.

Resumo

A busca de sistemas eficazes de administração de medicamentos tem sido alvo de investigação nas últimas décadas. Devido às muitas barreiras fisiológicas do corpo e à necessidade urgente de maior disponibilidade de medicamentos, a administração e efeito eficiente terapêutico de um medicamento tornaram-se num grande e importante desafio atualmente. A administração transdérmica de medicamentos ganhou recentemente muita atenção neste campo sendo maioritariamente limitada pela barreira da camada córnea. Muitos estudos foram conduzidos com o intuito de melhorar a permeação de um fármaco através da pele e muitos adesivos transdérmicos estão agora disponíveis para uso comercial devido à sua comodidade e propriedades não-evasivas. Neste trabalho, um sistema eutético terapêutico projetado para ser eficaz na administração de ibuprofeno através da pele foi incorporado numa membrana polimérica fibrosa produzida pelo método de *Solution Blow Spinning*. Efetuou-se a otimização da produção de membranas fibrosas, estudou-se o impacto dos parâmetros do método *Solution Blow Spinning* no diâmetro das fibras, avaliou-se a capacidade de retenção de fármaco das membranas, bem como a eficiência de reticulação UV e a resistência mecânica das membranas obtidas. O método *Solution Blow Spinning* mostrou-se simples e eficiente na produção de fibras micrométricas com diâmetros médios situados entre 1 e 5 μm . As membranas obtidas mostraram-se capazes de reter o fármaco eutético, mas são bastante frágeis e uma libertação controlada não foi conseguida devido à alta solubilidade do polímero usado na água.

List of acronyms

SBS – Solution Blow Spinning

DES – Deep Eutectic Solvent

THEDES – Therapeutic Deep Eutectic Solvent

MFD – Mean fiber diameter

SEM – Scanning Electron Microscopy

Abs – Absorbance

UV-Vis – Ultraviolet-Visible

PVP – Polyvinylpyrrolidone

PEG – Polyethylene glycol

TDDS – Transdermal drug delivery system

API – Active pharmaceutical ingredient

MO – Optical Microscopy

Mw – Molecular weight

PBS – Phosphate Buffer Saline

List of symbols

g – gram

mL – milliliter

nm – nanometer

μm – micrometer

$^{\circ}\text{C}$ – Celsius degrees

Da – Dalton

w/v – weight per volume

h – hour/s

cm – centimeter

L – Liter

C^* – Overlap Concentration

E – Young Modulus

ε – molar absorptivity coefficient

l – light path length

C – Concentration

Content

Chapter 1 Introduction	1
1.1. Polymers and Drug Delivery	1
1.2. Solution Blow Spinning (SBS)	1
1.3. Transdermal Drug Delivery	3
Chapter 2 Materials and Methods	7
2.1. PVP/DES solutions	7
2.2. Solution Blow Spinning (SBS)	7
2.3. UV crosslinking and swelling	7
2.4. Optical Microscopy (MO) and Scanning Electron Microscopy (SEM)	7
2.5. UV-VIS Spectroscopy in Drug Delivery	8
2.6. Mechanical assays	8
2.7. Rheology of the polymeric solutions	8
Chapter 3 Results and discussion	9
3.1. Fiber production and optimization	9
3.2. Rheological behaviour of polymeric solutions	13
3.3. Polymer concentration impact on fiber diameter	14
3.4. DES concentration impact on fiber diameter	16
3.5. Solution flow rate impact on fiber diameter	17
3.6. Air pressure impact on fiber diameter	18
3.7. Drug delivery	20
3.8. UV Crosslinking and Swelling capacity	21
3.9. DES distribution analysis	24
3.10. Mechanical tests	25
Chapter 4 Conclusions and future perspectives	28
Chapter 5 References	31

Chapter 6 Attachments	35
6.1. Polymeric solutions preparation	35
6.2. MFD values resulting from SBS optimization study	36
6.3. Ibuprofen calibration curve.....	37
6.4. PBS solution recipe.....	37
6.5. DES molecular weight and density.....	38

List of figures

Figure 1: A schematic of an Electrospinning process (Huang et al., 2003).	2
Figure 2: An schematic of a SBS montage (left); the fiber jets formation at the nozzle exit (top right) and some examples of fibers obtained by a SBS method (down right) (Greenhalgh et al., 2017; Medeiros et al., 2009).	3
Figure 3: Possible pathways for drug permeation through the skin (left) and through the Stratum Corneum (right) (Benson, 2005; Hadgraft, 1979).	4
Figure 4: Skin Permeation Enhancement/Optimization Techniques (Benson, 2005).	4
Figure 5: Optical microscopy images of a PVP membrane produced out of a 10% PVP concentration solution.	10
Figure 6: SEM image of a 14% pure PVP membrane.	11
Figure 7: SBS setup schematic.	11
Figure 8: SEM images of 14% PVP + 0.5% DES (left) and 16% PVP + 0.5% DES (right).	12
Figure 9: SEM imagens of a 18% PVP membrane (top left), a 20% PVP membrane (top right) and a 22% PVP membrane (bottom).	13
Figure 10: a) Flow curves of the 18% PVP solutions; b) Flow curves of the 20% PVP solutions. All assays were performed at 5°C.	14
Figure 11: Samples of a 18% PVP membrane (left) and a 20% PVP membrane (right)	15
Figure 12: Fiber diameter distribution for the different polymer concentrations and respective statistical results gathered for the 18% concentration (bottom left) and 20% concentration (bottom right).	15
Figure 13: Fiber diameter distribution for the different DES concentrations and respective statistical results gathered.	17
Figure 14: Obtained SEM imagens of 18% PVP with 0.5% DES (top left), 1% DES (top right) and 2% DES (bottom).	17
Figure 15: Fiber diameter distribution and respective statistical results for the used solution flow rates of 5 mL/h (left) and 6 mL/h (right).	18
Figure 16: Fiber diameter distribution for the used air pressures and respective statistical results gathered for the 2.5 bar (bottom left) and 3 bar (bottom right).	19
Figure 17: Representation of the final structure of the obtained membranes.	20
Figure 18: UV crosslinking of polymeric membrane at irradiation chamber.	21

Figure 19: Illustration of the approach taken into analysing DES distribution through the PVP membrane. 24

Figure 20: Absorbance values in each site for each DES concentration (left) and average absorbance relation with the zone of the analysed membranes (right)..... 25

Figure 21: Obtained Stress/Strain graphs for each DES concentration membrane. 26

Figure 22: Obtained calibration curve for ibuprofen release in aqueous medium. 37

List of tables

Table 1: Used concentrations of PVP and DES.	7
Table 2: Range of operation of SBS parameters.	14
Table 3: The best determined parameters conditions for the SBS setup.	20
Table 4: Swelling capacity results of tested membranes.	22
Table 5: Results of the delivery of ibuprofen into PBS at room temperature.	23
Table 6: Obtained Young modulus for each membrane.	27
Table 7: Some experimental values of the measured mass of PVP for 18% PVP concentration.	35
Table 8: Some experimental values of the measured mass of DES for 0.5% DES concentration.	35
Table 9: Some experimental values of the measured mass of DES for 1% DES concentration.	35
Table 10: Some experimental values of the measured mass of DES for 2% DES concentration.	35
Table 11: Some experimental values of the measured mass of PVP for 20% PVP concentration.	35
Table 12: MFD for all variations done during the SBS process.	36
Table 13: Ibuprofen calibration curve parameters.	37
Table 14: PBS recipe components.	37
Table 15: Mass values of each sample measured.	38

Chapter 1 Introduction

The development of effective treatments for diseases has been a major goal of humanity ever since. Over time, we have greatly improved our understanding of the human body and the functions of its various cooperating systems as well as the living cells that constitute their building blocks. The acquired knowledge has led to the development of a great variety of therapeutics, both natural and synthetic, to fight against infectious diseases, inflammatory illnesses, physical or mental disorders, and malfunctions of the body's components. More than the drugs itself, we have been lately improving the delivery methods (Ulbrich et al., 2016).

Although conventional drug delivery formulations have contributed greatly to the treatment of diseases, the emergence of new, potent and specific biological therapeutics has escalated the impetus for intelligent delivery systems. These systems must overcome many hurdles before clinical implementation is realized; a truly intelligent delivery system must address the need for specific targeting, intracellular transport, and biocompatibility while integrating elements of responsive behaviour to physiological environments (Liechty, Kryscio, Slaughter, & Peppas, 2010).

1.1. Polymers and Drug Delivery

Polymers have played an integral role in the advancement of drug delivery technology and have been tailored for modify transport or circulation, half-life characteristics, to allow for passive and active targeting and engineered to exert distinct biological functions. Such polymers have largely included cellulose derivatives, PEG (polyethylene glycol), and PVP (poly-N-vinylpyrrolidone) (Rowe, Sheskey, & Quinn, 2009). As a water soluble synthetic polymer, PVP has many desirable properties including low toxicity, chemical stability, and good biocompatibility. It is also hemocompatible, physiologically inactive, non-irritating to skin, eye, and mucous membrane being used in many biomedical applications such as membranes, adhesives, ceramics, coatings and as a blood plasma substitute (Haaf, Sanner, & Straub, 1985; Liechty et al., 2010; Liu, Xu, Wu, & Chen, 2013; Smith, Rimmer, & MacNeil, 2006; Teodorescu & Bercea, 2015).

1.2. Solution Blow Spinning (SBS)

Polymeric micro and nanofibers production technology have gained wide interest because of its unique properties compared to larger diameter fibers made of the same material. Decreasing the diameter of fibers to the nanoscale markedly increases the surface area to volume ratio, increases liquid holding capacity, and changes texture and appearance. Nanofibers hold great promise for medical uses such as for tissue engineering scaffolds, controlled release of drugs and medications and as wound dressing for skin

regeneration (Huang, Zhang, Kotaki, & Ramakrishna, 2003; Ramakrishna, Fujihara, Teo, Lim, & Ma, 2005).

Electrospinning (figure 1) of polymers was first reported with increasing intense research activity in recent years because of its adaptability to a wide range of polymeric materials and its consistency in producing very fine fibers. In the electrospinning process, an electrical charge is applied to a polymeric solution. At a point where the electrical forces created by the repulsion of positive charges on the solution overcomes the forces of surface tension, a fluid jet erupts and travels to a grounded collector. The high surface to volume ratio of the jet facilitates rapid evaporation of the solvent component and results in fine fibers that are randomly formed and can be collected to form a non-woven web (Huang et al., 2003; Ramakrishna et al., 2005).

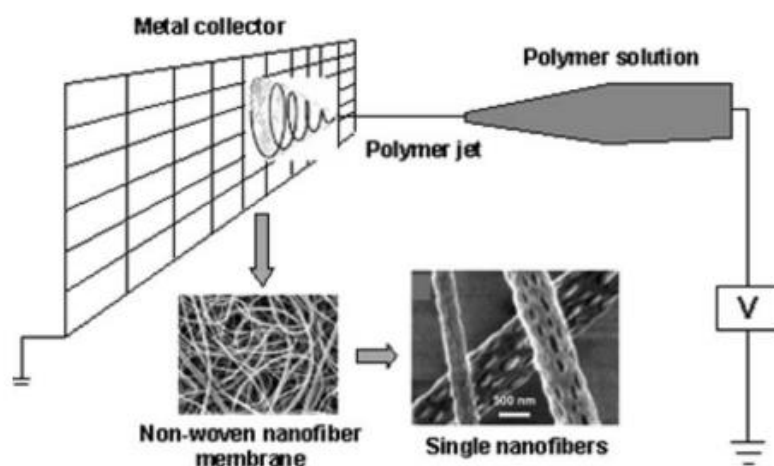


Figure 1: A schematic of an Electrospinning process (Huang et al., 2003).

Even though electrospinning is considered the technique with the most potential for scaling to commercial production, the solvents that are compatible with the electrospinning process may be limited by their dielectric constant.

SBS (figure 2) is a simple and rapid technique to produce nanofibers, using pressurized air-stream as driving force for fiber formation. The high velocity airflow used in SBS aids solvent evaporation for dry fiber production. Most published work on solution blow spinning involves the use of highly volatile organic solvents (or solvent mixtures). Spinning from low volatile solvents like water is challenging since the fibers may not fully dry before reaching the collector resulting on fiber defects (Daristotle, Behrens, Sandler, & Kofinas, 2016; Santos, Medeiros, Blaker, & Medeiros, 2016).

SBS overcomes some drawbacks associated with the electrospinning process such as the use of an electric field. The method is therefore easily implemented using inexpensive, transportable, and handheld equipment. SBS allows for scalable production and deposition at the point and site of interest making this a reliable technique for emergency depositions. Applications of SBS in biomedical engineering are highlighted, showing enhanced cell infiltration and proliferation versus electrospun fiber scaffolds and

in situ deposition of biodegradable polymers (Daristotle et al., 2016; Medeiros, Glenn, Klamczynski, Orts, & Mattoso, 2009; Santos et al., 2016).

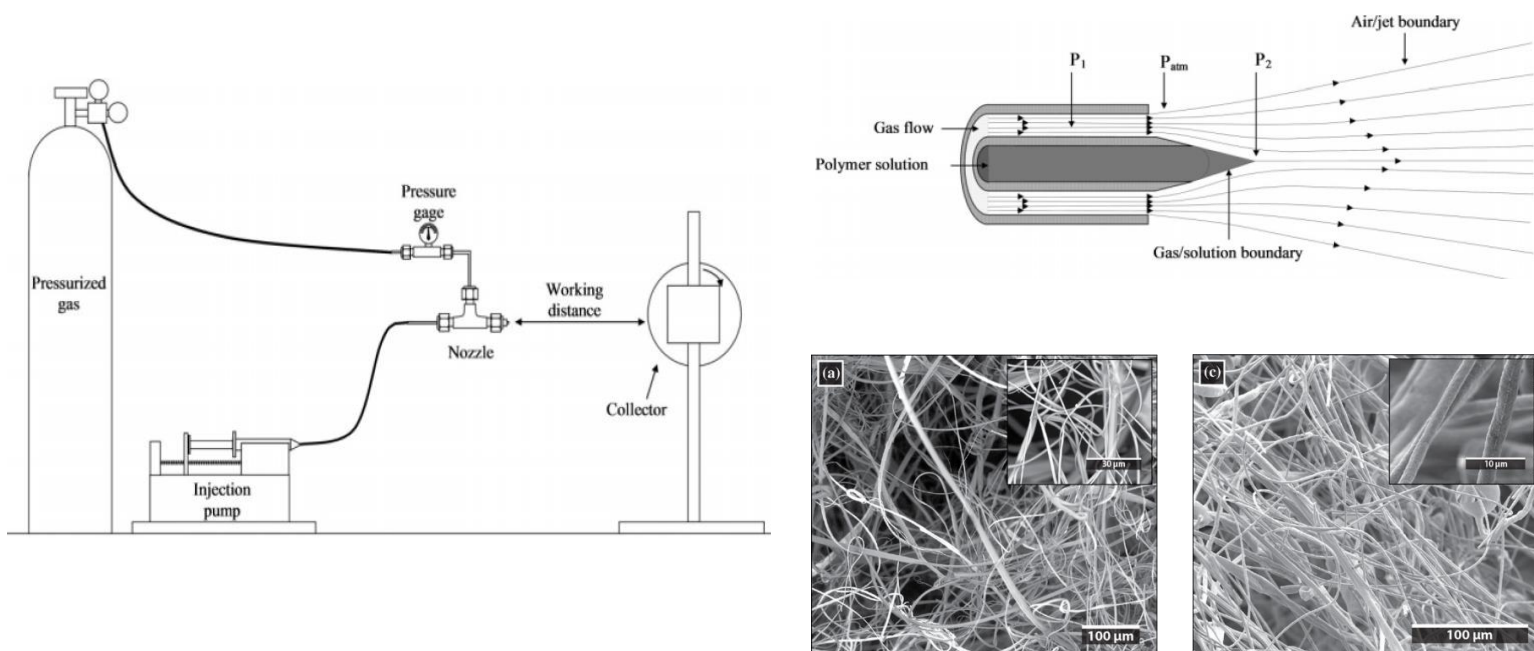


Figure 2: An schematic of a SBS montage (left); the fiber jets formation at the nozzle exit (top right) and some examples of fibers obtained by a SBS method (down right) (Greenhalgh et al., 2017; Medeiros et al., 2009).

1.3. Transdermal Drug Delivery

Conventional drug delivery methods as oral and parenteral administration have limitations regarding physiological barriers through which the drug must pass. A transdermal drug delivery system (TDDS) is an appealing alternative to minimize and avoid the limitations allied with these drug administration methods. It consists in the permeation of drugs through the skin, into the systemic circulation, in a proper and prolonged steady-state delivery, avoiding the hepatic first-pass effect and reducing prospects of other side effects enhancing therapeutic efficacy (Barry, 1991; Kalluri & Banga, 2011).

Polymers are utilized in TDDS in versatile manners of transdermal patches including as: rate-controlling membranes, adhesives, backing layers, and release liners. These patches are extremely commodious, user-friendly and provide the ease of termination if need arises (Alexander et al., 2012).

The intact skin is a tough barrier and there are a lot of skin conditions affecting drug percutaneous absorption like solubility, lipophilicity, molecular weight or size, and hydrogen bonding. One of the most important factors is the intrinsic solubility of drug in the skin, this is closely related to the melting point of the drug, the membrane density and molecular weight, drug molecular weight and its entropy of fusion (Benson, 2005; Stott, Williams, & Barry, 1998).

Drug molecules in contact with the skin surface can penetrate by three potential pathways: through the sweat ducts, via the hair follicles and sebaceous glands (collectively called the shunt or appendageal route), or directly across the stratum corneum (figure 3).

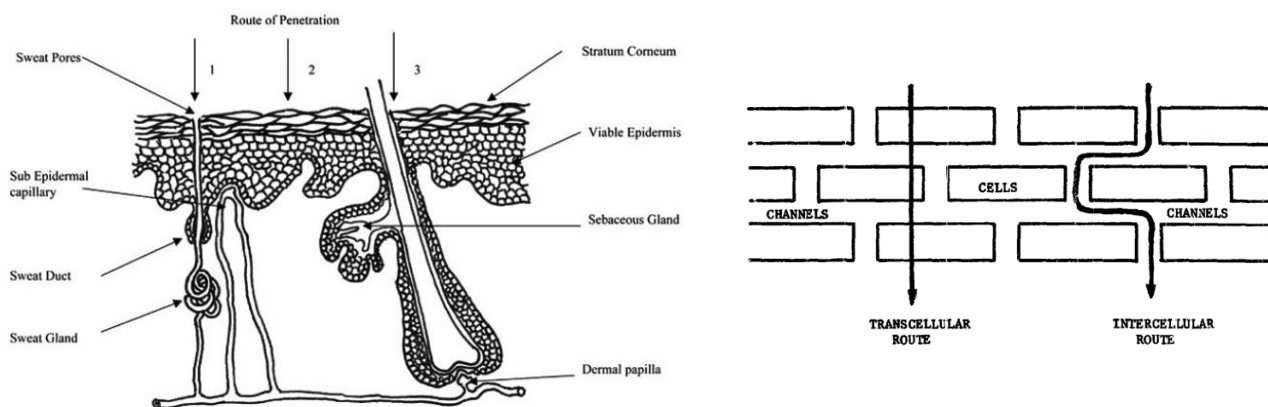


Figure 3: Possible pathways for drug permeation through the skin (left) and through the Stratum Corneum (right) (Benson, 2005; Hadgraft, 1979).

Even though it is known that permeation through the follicular shunt route most likely offers a steady-state profile rather than the stratum corneum, the responsible appendages comprise a very small fractional area of about 0.1% and so their contribution to steady state flux of most transdermal drugs is minimal. This is why the majority of skin penetration enhancement techniques have been focused on increasing transport across the stratum corneum rather than via the appendages (Benson, 2005).

Studies have shown that a reduction in the melting point of a permeant, which has been shown to be inversely proportional to lipophilicity, will increase its solubility in skin lipids and so increase transdermal permeation. So, if one can reduce the melting point of a drug without causing unfavourable changes to other physicochemical parameters, then this should enhance transdermal flux. As for the molecular weight is rather simple, as smaller the molecular weight (ideally less than 500 Da), easier is for the drug to permeate through the skin (Benson, 2005; Stott et al., 1998).

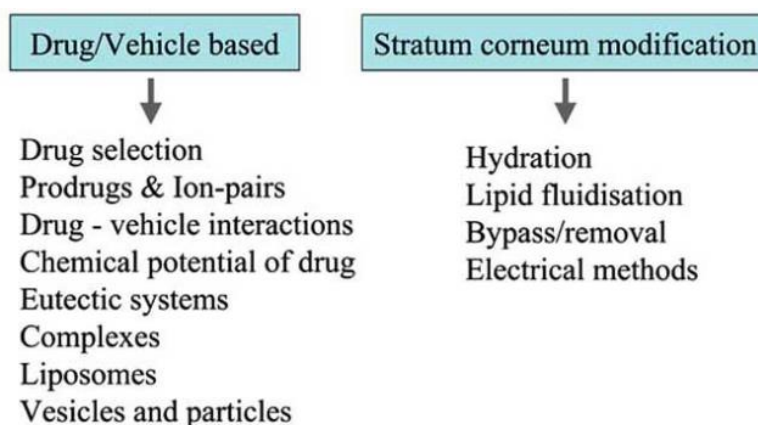


Figure 4: Skin Permeation Enhancement/Optimization Techniques (Benson, 2005).

As shown in figure 4, one of the ways to reduce melting point of a substance is by eutectic formation. An eutectic is a substance generally composed of two or three solid, cheap and safe components that are capable of self-association, often through hydrogen bond interactions, to form a mixture with a resulting melting point lower than that of each individual component. These are generally liquid at temperatures lower than 100°C and they are called of Deep Eutectic Solvents (DES) (Benson, 2005; Stott et al., 1998).

It is possible to form a DES with an active pharmaceutical ingredient (API) and therefore increase the solubility, permeation and absorption of the API through the skin (Aroso et al., 2016; Stott et al., 1998). Those DES, which possess an API, are called THEDES (Therapeutic Deep Eutectic System).

This work comes to report the optimization of the production of non-woven polymeric membranes of PVP impregnated with a THEDES using a coaxial SBS method. The THEDES used is a 3:1 molar ratio menthol:ibuprofen eutectic system in which the ibuprofen is the API and menthol is a well-recognized skin permeation enhancer (Babu & Pandit, 2005; Kunta, Goskonda, Brotherton, Khan, & Reddy, 1997). A study that came to analyse SBS parameters influence in fiber diameter will be presented. Furthermore, mechanical, swelling and DES release properties of the obtained membranes have been also studied.

Chapter 2 Materials and Methods

2.1. PVP/DES solutions

PVP (Sigma Aldrich, Mw = 1.300.000) dissolved in ethanol (Sigma Aldrich, 96%) solutions were used for fiber production. The solutions were prepared by dissolving different weight per volume (w/v) percentages of PVP into ethanol and magnetically stirred for 1h at room temperature until complete homogenization was achieved. Then the menthol:ibuprofen of 3:1 molar ratio DES was added also in weight per volume percentages and the final solution would remain at stirring for 2 more hours before use. Table 1 contains the used concentrations for PVP and DES in this work.

Table 1: Used concentrations of PVP and DES.

PVP Concentrations (w/v %)	6, 8, 10, 12, 14, 16, 18, 20, 22
DES Concentrations (w/v %)	0.5, 1, 2

2.2. Solution Blow Spinning (SBS)

The SBS experiments were conducted using Linari 2 layers sealed coaxial system (COAX_2DISP), a digitally programmed syringe pump (kdScientific), a Nitrogen bottle as air supplier and a homemade rotative collector. The pump allowed to obtain solution flow rates ranging between 4 and 8 mL/h. As for the Nitrogen bottle, it allowed for consistent and regulated air pressures of 1; 2; 2.5 and 3 bar. The process was performed in open environment at room temperature with working distances (nozzle tip to collector distance) ranging between 15 and 20 cm.

2.3. UV crosslinking and swelling

The fibrous membranes were crosslinked with 254 nm ultraviolet light in a BIO-LINK® irradiation system. The membranes were irradiated for 50 min (Faria, 2016). After the crosslinking, 3 pieces of each membrane for each DES concentration of 1 cm × 1 cm dimensions were cut and submerged into 2mL of distilled water. The samples were left at 50°C during 24h.

2.4. Optical Microscopy (MO) and Scanning Electron Microscopy (SEM)

Both MO and SEM were performed in order to analyse fiber morphology. For the SEM analysis, small pieces of the fibrous membranes were fixed on carbon tape and then mounted on a aluminium support to be sputtered with a thin layer of gold using a Q300T D Quorum sputter coater. The samples were analysed by a Zeiss DSM 962 scanning electron microscope. As for the MO analysis, fibrous membranes were directly deposited in glass covers that allowed them to be observed in a OLYMPUS BX 51 microscopy. The

diameter distribution of the obtained fibres was determined by using FIJI ImageJ software.

2.5. UV-VIS Spectroscopy in Drug Delivery

A T90+ UV/VIS Spectrophotometer from PG Instruments Ltd spectroscopy apparatus was used to analyse the drug delivery profile of the produced membranes. The delivery medium was a PBS (Phosphate Buffered Saline) solution adjusted for a 7.4 pH produced according a protocol offered by AAT Bioquest®. The used recipe data can be consulted in the section 6.4 of this work.

The objective was to detect ibuprofen and so the wavelength of detection was set to 264 nm. First, in order to evaluate the ibuprofen release over time, samples of an entire membrane, for each DES concentration, submerged in 20 mL of PBS under magnetic stirring at 37°C of temperature were collected at different times. Same procedure was made for crosslinked membranes. Then, five pieces of each non-crosslinked membranes were submerged in 2mL of PBS until its full dissolution and then collected. All samples collected were stored in eppendorfs and two quartz cuvetts of 1 cm x 1 cm dimensions were used to place the samples into the spectrophotometer. The observation range was defined to be between 240 and 280 nm of wavelength.

2.6. Mechanical assays

Stress/Strain tests were performed in order to study non-woven mats mechanical behaviour. Three membrane samples were cut in small rectangular pieces of around 3 cm length and 1 cm width, mounted between a pair of iron clamps of a Rheometric Scientific, Minimat Firmware 3.1 machine and then stretched at a speed of 1 mm/min.

2.7. Rheology of the polymeric solutions

The shear viscosities of the stock solutions were measured at 25°C, in a shear range of $10^{-2} - 10^2 \text{ s}^{-1}$ using a Bohlin Gemini HRnano rotational rheometer equipped with a 40 mm plate fixtures. The plate compressed the polymeric solutions up to a gap of 500 μm and then applying a pre-shear to ensure a steady state.

Chapter 3 Results and discussion

3.1. Fiber production and optimization

One of the main objectives of this dissertation was to optimize the production of PVP fibrous membranes impregnated with a menthol:ibuprofen DES by using the SBS method. To do so, parameters like: polymer concentration, working distance, solution flow rate and air pressure were varied in specific range of values with the intention of achieving the lowest mean fiber diameter (MFD). The solvent used in the polymeric solutions was ethanol since it shown that can effectively dissolve both PVP and the DES simultaneously. In this work, all concentrations of both these components were weight/volume (w/v – g/mL) percentages.

The ability to form fibers from a jet of polymer solution is primarily governed by the entanglement of polymer chains. It is known that concentration is proportional to fiber diameter and that this should be superior to the overlap concentration (C^*) of the used polymer. The overlap concentration represents the critical point when polymer coils in solution begin to overlap, causing entanglements. Experiments have confirmed that SBS forms fibers when polymer concentration is superior to C^* ($C > C^*$), “beads-on-a-string” near C^* ($C \sim C^*$), and corpuscular morphologies below C^* ($C < C^*$). For the PVP with $M_w = 1300000$ g/mol, the overlap concentration value is around of 0.7% w/v (Yu, 2017). The air pressure and solution flow rate are dependant of viscosity of the polymeric solution and therefore of the polymer concentration. A higher solution viscosity needs a higher solution flow rate in order to prevent nozzle clogging and a bigger air pressure to be blown away forming fiber jets. The balance between air pressure and solution flow rate depends of the nature of the solvent and the polymer used. Fiber diameter is only affected by polymer solution flow rate at low gas pressures. However, low and high feed rates may cause jet instability or nozzle clogging, respectively. Increasing gas pressure produces a narrower fiber diameter distribution with less variance and consistent fiber morphology. However, increasing gas flow rate beyond the optimal range may also cause a temperature decrease around the polymeric jet which may cause poor solvent evaporation and fiber welding (Daristotle et al., 2016).

At the work first stages, it was critical to determine the minimal polymer concentration which would allow for fiber formation using this method, polymeric solutions based only on PVP with concentrations of 6, 8 and 10% (w/v) were chosen to start the production. The solution flow rate was set to 6 or 8 mL/h, the air pressure set to 1 or 2 bar and the working distance was fixed at 15 cm. PVP is a very hydrophilic polymer and, for these initial concentrations, only the 10% polymer concentration has allowed for well-defined fiber formation (figure 5), being the obtained membranes stewed with ethanol.

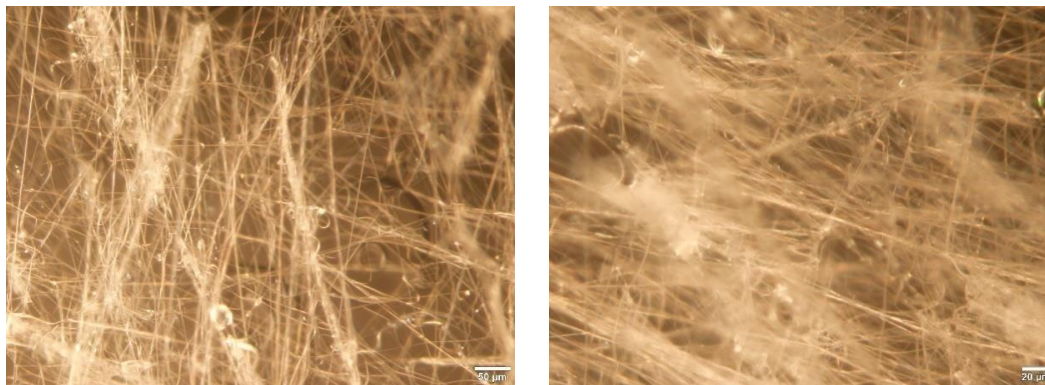


Figure 5: Optical microscopy images of a PVP membrane produced out of a 10% PVP concentration solution.

When the first set of fibers was obtained, the first polymeric solutions with DES were made using the concentrations of 0.5%, 1% and 2% w/v. Using the same experimental conditions mentioned before, no effective fiber formation has been observed. It looked like the solvent was not properly evaporating resulting in a spray of polymeric residuals. To force solvent evaporation, polymer concentration and working distance were increased until good fiber formation was achieved. Polymer concentration was increased with a 2% increment, first to 12 and 14% using a working distance of 20 cm.

For the polymer concentrations of 12 and 14%, air pressures changing between 1 or 2 bar, solution flow rates of 6 or 8 ml/h at a fixed working distance of 20 cm, good fiber formation was achieved for pure PVP (figure 6). Some other studies showed that, for the same system of PVP/ethanol, using very similar conditions as the ones mentioned before also resulted in good fiber formation and that, for pure PVP, this were most likely to be the best concentration range in order to achieve the smallest mean fiber diameter (Zhang, Kopperstad, West, Hedin, & Fong, 2009.).

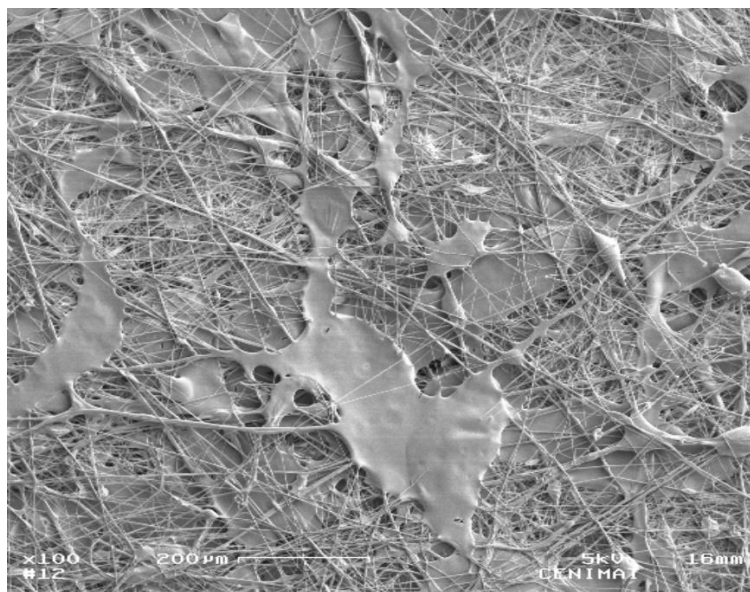


Figure 6: SEM image of a 14% pure PVP membrane.

When the DES was added to the polymeric solutions of 12 and 14% PVP w/v respectively, once again, there was more of a spray than fiber formation due to poor solvent evaporation. To solve the current problem, it was chosen to increase the environment temperature in order to improve solvent evaporation. A hair dryer was added to the SBS montage (figure 7) which created a surrounding hot air stream that set the outer temperature of the nozzle, from which the polymeric solution flowed, to approximately 50°C.

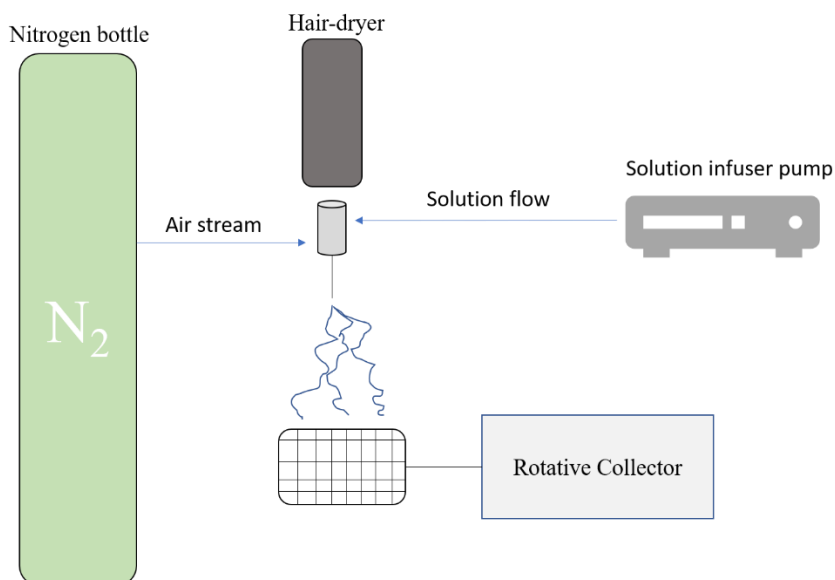


Figure 7: SBS setup schematic.

The hair dryer came to increase solvent evaporation and therefore fiber formation. However, the presence of agglutinated fiber domains dominated the area of the samples collected and analysed by SEM. This was most likely due to contact between the solution

jets before solvent was completely evaporated (Zhang et al., 2009.). The solution used to approach this issue was to increase even more the polymer concentration to values of 16, 18, 20 and 22% w/v of PVP.

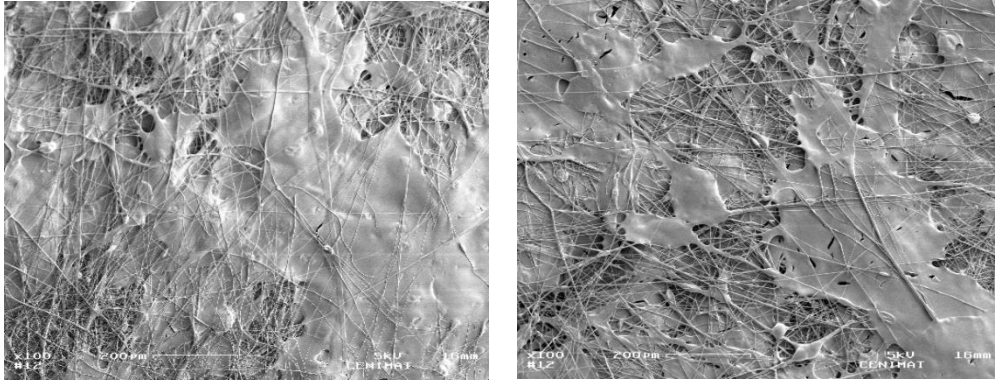


Figure 8: SEM images of 14% PVP + 0.5% DES (left) and 16% PVP + 0.5% DES (right).

Of these conditions, as it is observed on figure 8, the 16% polymer concentration shown yet to be ineffective at reducing fiber agglutination as the 18% proved to be the overall best, the 20% the second best and the 22% really unnecessary (figure 9) since, for most of the experiments made, the nozzle would constantly clog due to its very high viscosity.

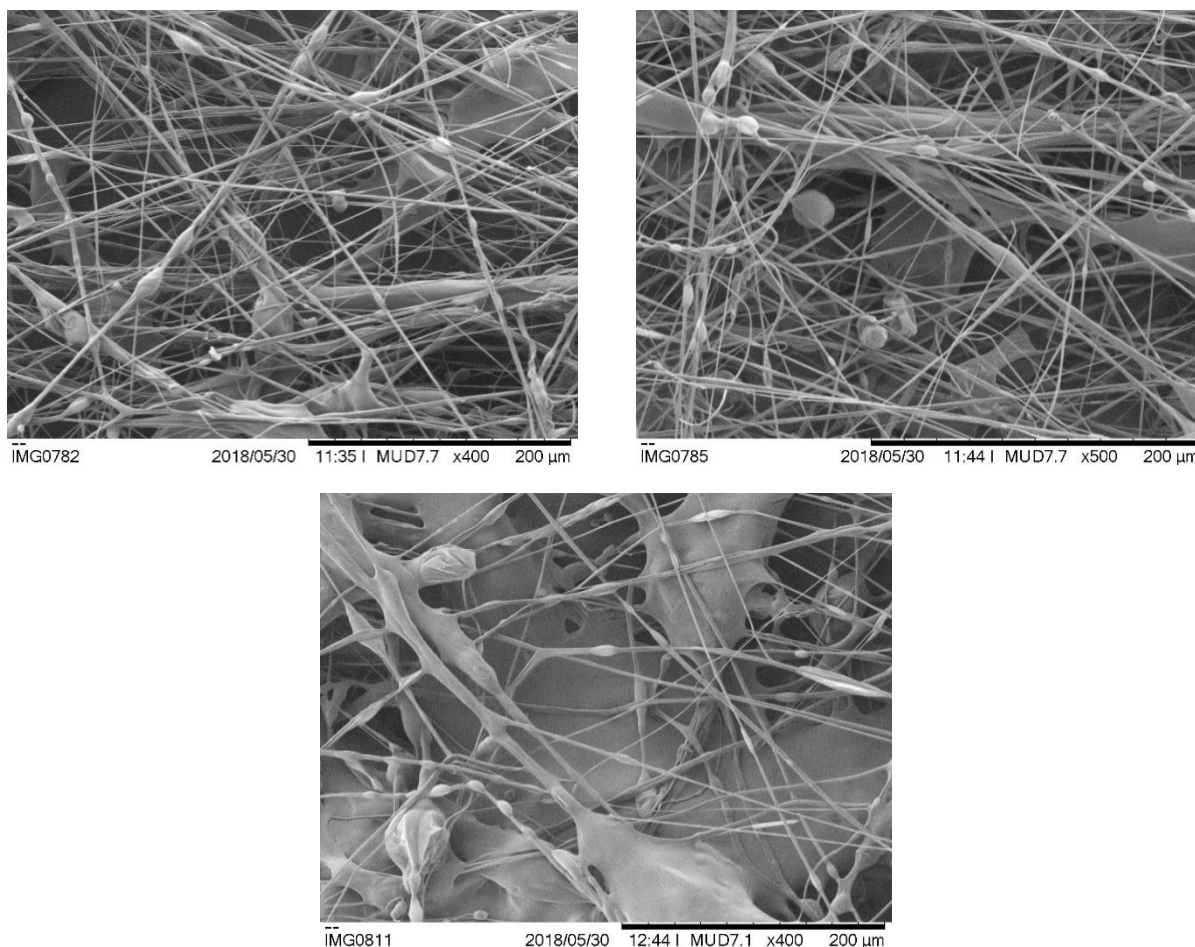


Figure 9: SEM images of a 18% PVP membrane (top left), a 20% PVP membrane (top right) and a 22% PVP membrane (bottom).

3.2. Rheological behaviour of polymeric solutions

It was clear that the DES caused some undesired effect that came to difficult solvent evaporation and therefore fiber formation, resulting in large domains of molten/agglutinated fibers. In order to test how the DES interacted with the polymeric solution, rheological studies were performed for the solutions of 18 and 20% PVP being the obtained results present in figure 10.

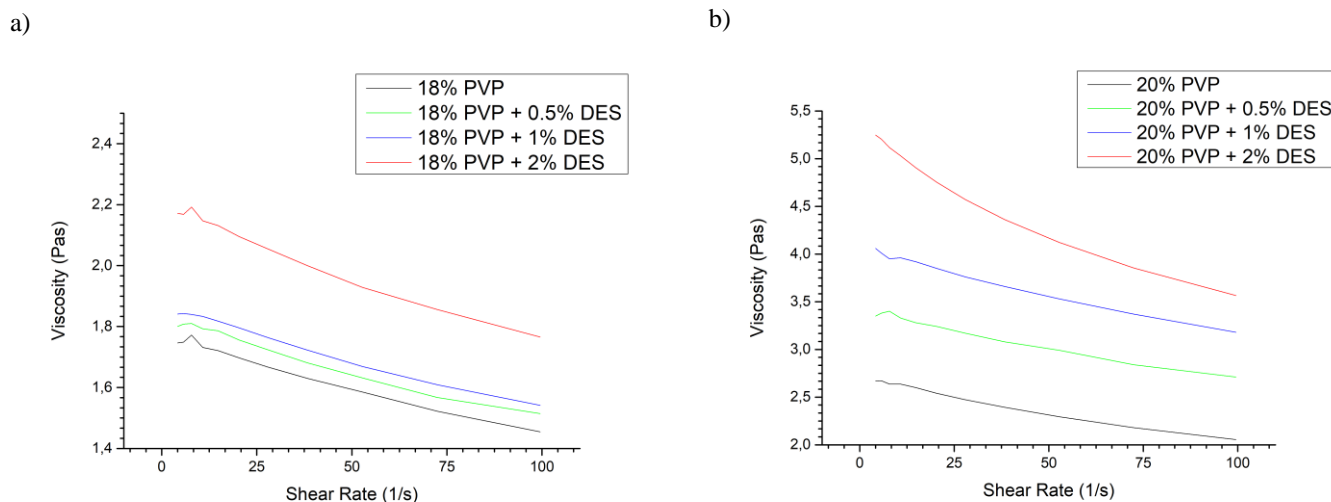


Figure 10: a) Flow curves of the 18% PVP solutions; b) Flow curves of the 20% PVP solutions. All assays were performed at 25°C.

By observing the obtained flow curves from the analysed samples, it is concluded that the obtained polymeric solutions exhibit a non-Newtonian behaviour typical of a pseudoplastic fluid with shear-thinning behaviour. In this kind of fluids, the viscosity decreases as the shear rate increases. This is caused by the structural reorganization of the fluid molecules due to the flow. Some common examples of pseudoplastics include ketchup, paints, even blood (Chhabra, 2010).

As for the DES, it came to severely increase solution viscosity when added, making its blowing more difficult. This could inhibit the formation of well-defined fiber jets resulting in fiber welding (Daristotle et al., 2016; Medeiros et al., 2009).

As mentioned before, the polymer concentration of 18% shown to be the best at ensuring the least of fiber welding at same time that keeps the lowest mean fiber diameter (MFD) possible. To support this affirmation, a study to analyse diameter variation and the impact of each operation parameter on diameter distribution was made. In this study, the different parameters were varied according to the values presented in table 2.

Table 2: Range of operation of SBS parameters.

Parameters	Range of operation
Polymer concentration	18%, 20% g/mL
DES concentration	0.5%, 1%, 2% g/mL
Solution flow rate	5, 6 mL/h
Air pressure	2.5, 3 bars
Distance to collector	20 cm

3.3. Polymer concentration impact on fiber diameter

The present section comes to present the obtained results of the polymer concentration impact in fiber formation and diameter. The data presented on figures 11

and 12 results of all the essays made for the 18% and 20% PVP concentrations respectively.

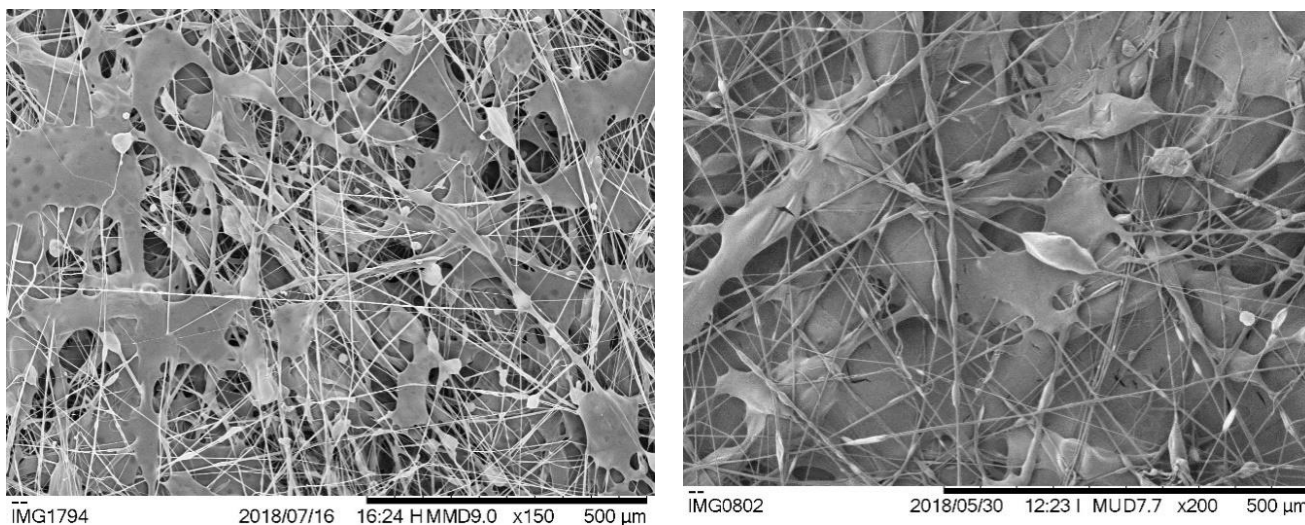
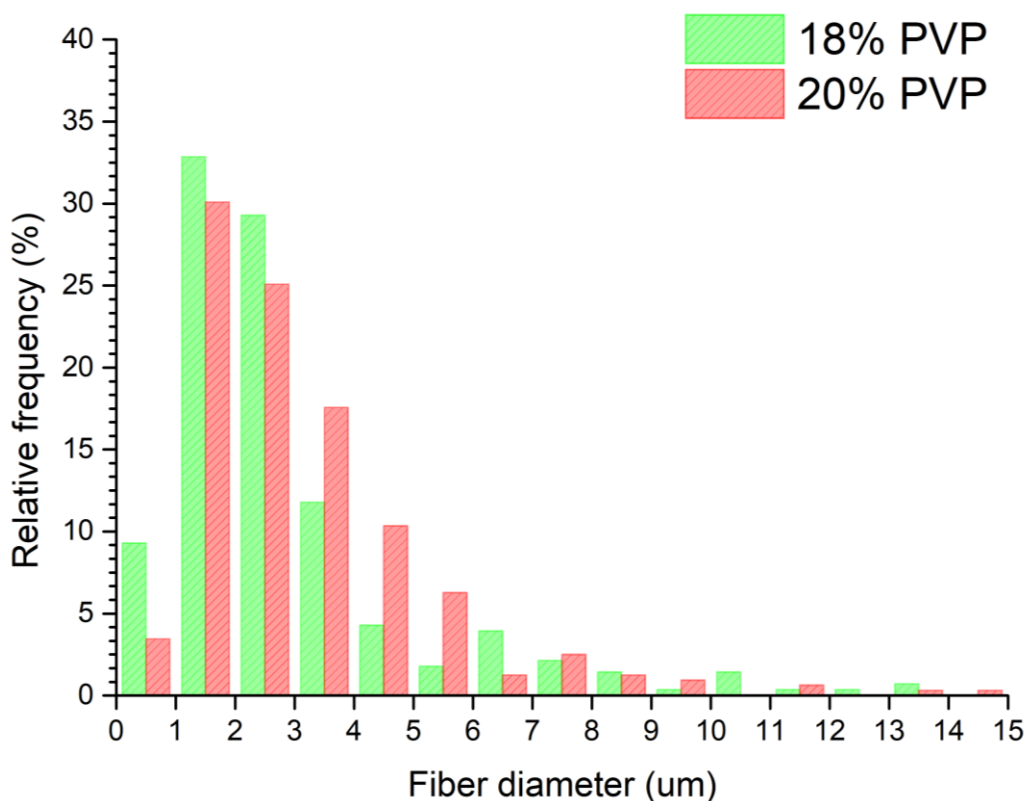


Figure 11: Samples of a 18% PVP membrane (left) and a 20% PVP membrane (right)



Mean	Standard Deviation	Minimum	Median	Maximum
2.911	2.284	0.340	2.237	13.830

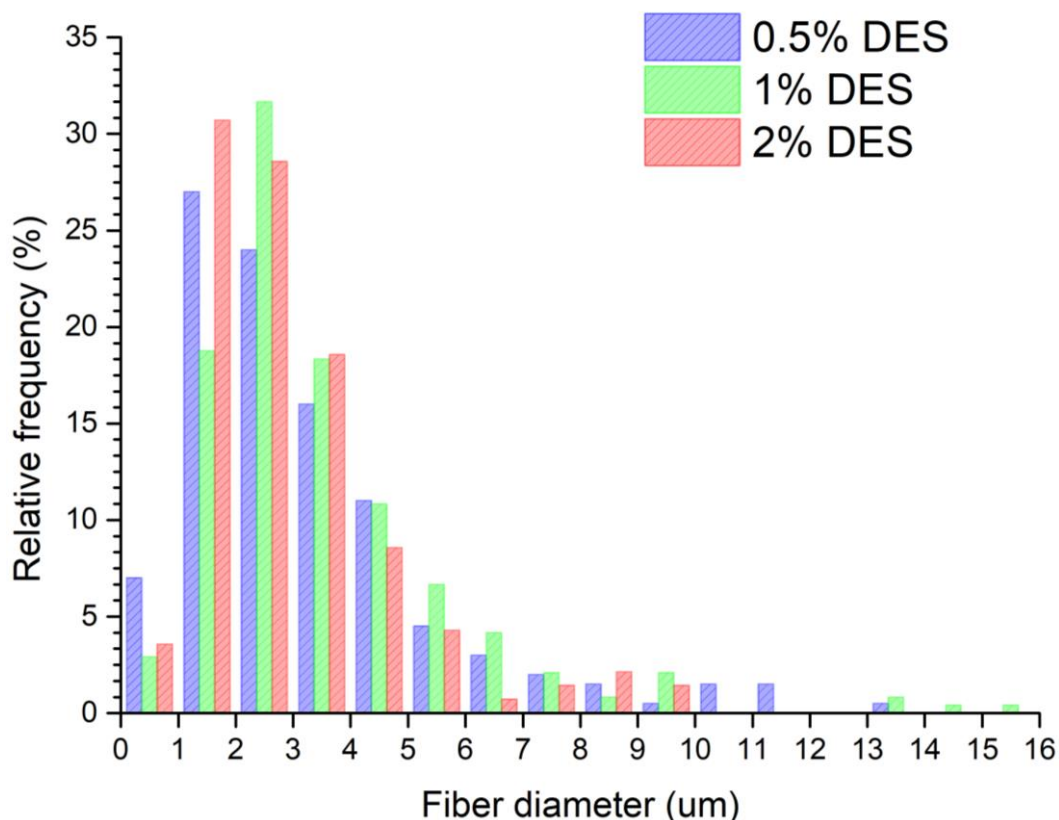
Mean	Standard Deviation	Minimum	Median	Maximum
3.139	2.019	0.549	2.563	14.373

Figure 12: Fiber diameter distribution for the different polymer concentrations and respective statistical results gathered for the 18% concentration (bottom left) and 20% concentration (bottom right).

As it is possible to see from figure 12, a smallest MFD of 2.91 μm was obtained for the concentration of 18%. As for the concentration of 20%, a MFD of 3.14 μm was measured. The overall obtained fibers were inserted in the micrometric domain having very few nanofibers as is typical of the SBS method (Zhang et al., 2009.). It has to be mentioned that the problem of the fiber welding was never fully solved and such might be impossible to this set of components.

3.4. DES concentration impact on fiber diameter

The following figure 13, presents the data related to the study of the impact that the DES had on fiber diameter for the used concentrations of 0.5, 1 and 2% respectively.



0.5% DES	Mean	Standard Deviation	Minimum	Median	Maximum
	3.271	2.319	0.454	2.594	13.031
1% DES	Mean	Standard Deviation	Minimum	Median	Maximum
	3.497	2.291	0.340	2.830	15.869
2% DES	Mean	Standard Deviation	Minimum	Median	Maximum
	2.940	1.782	0.641	2.548	9.432

Figure 13: Fiber diameter distribution for the different DES concentrations and respective statistical results gathered.

According to the results gathered and FTIR-ATR assays of the used polymeric solutions, there are not any signs of interactions between the eutectic substance and the polymeric chains, it is expectable that the DES has no significant impact on diameter of obtained fibers and that it comes only to cause jet instability resulting on fiber welding. This can be confirmed by the presented data in figure 13 and on figure 14 which shows that, for a fixed polymer concentration, the increase of DES concentration results in a decrease of fiber formation.

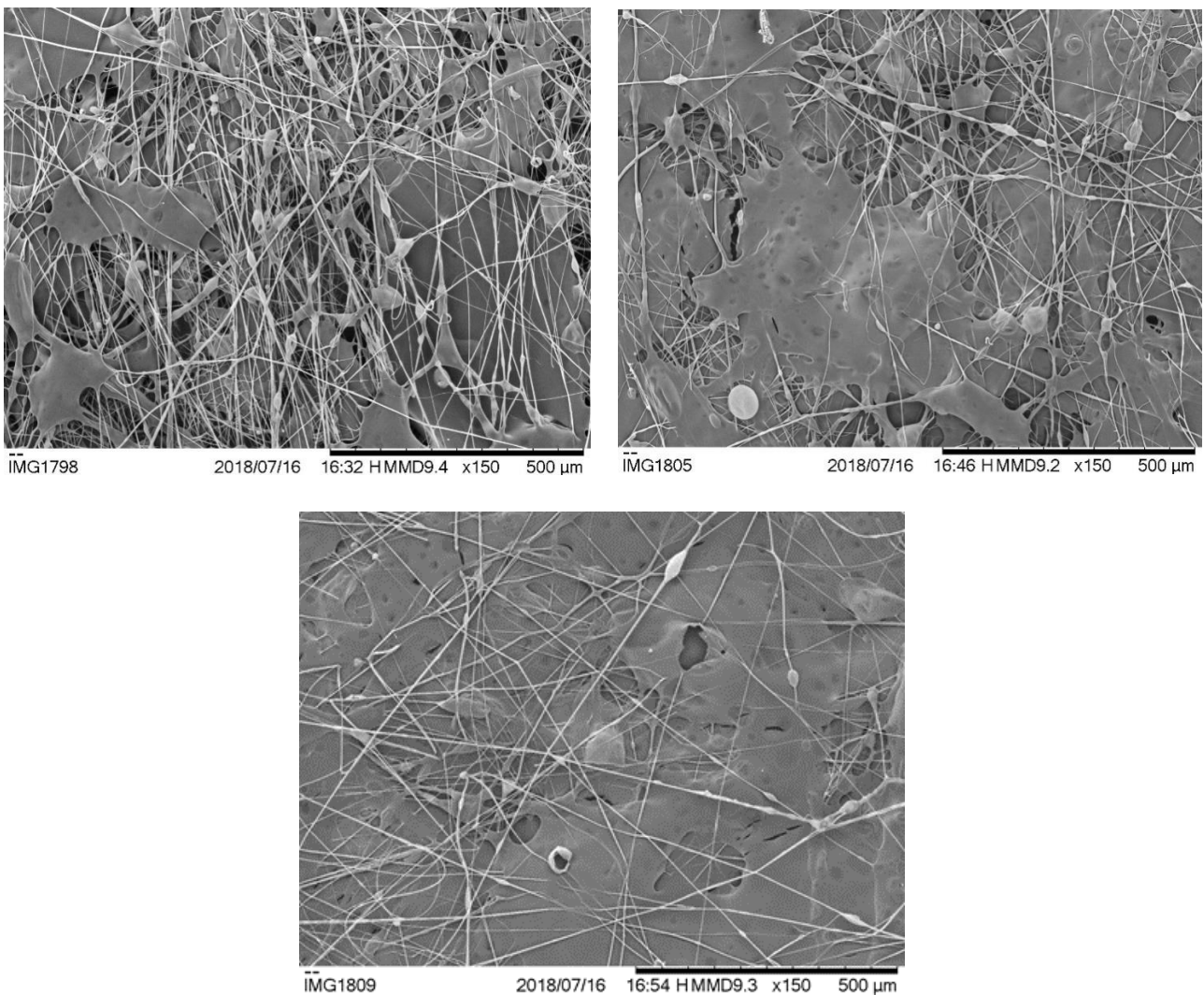
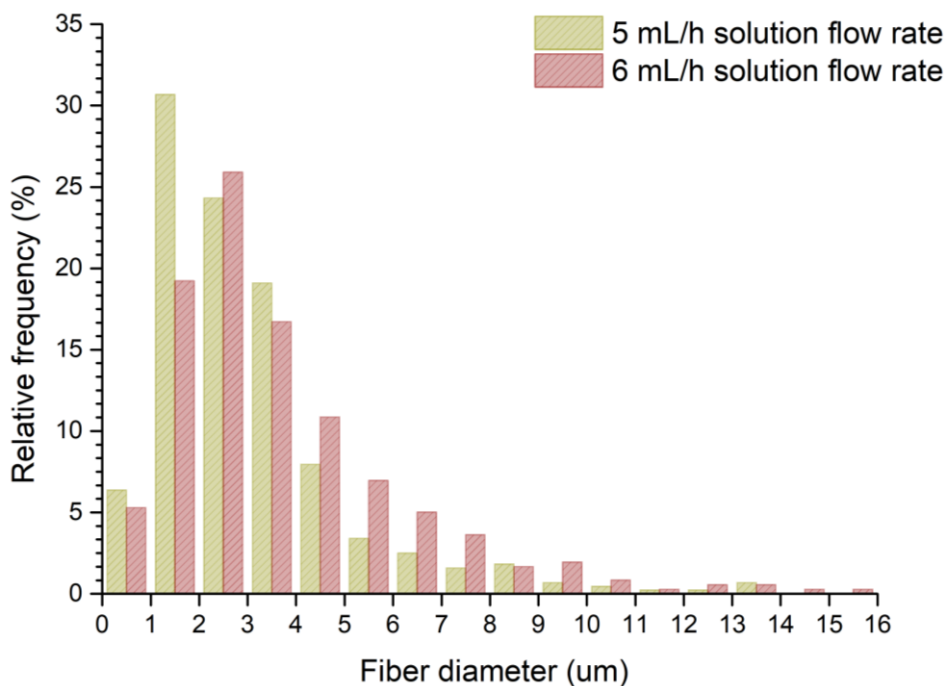


Figure 14: Obtained SEM images of 18% PVP with 0.5% DES (top left), 1% DES (top right) and 2% DES (bottom).

3.5. Solution flow rate impact on fiber diameter

The solution flow rate does not really have a direct impact on fiber diameter but if too much increased, because there is a greater volume of solution to be blown away, might result in incomplete solvent evaporation and jet instability therefore resulting in defects

among the fibers (Daristotle et al., 2016; Faria, 2016). The statistical results obtained for the impact of the used solution flow rates on fiber diameter are presented in figure 15.



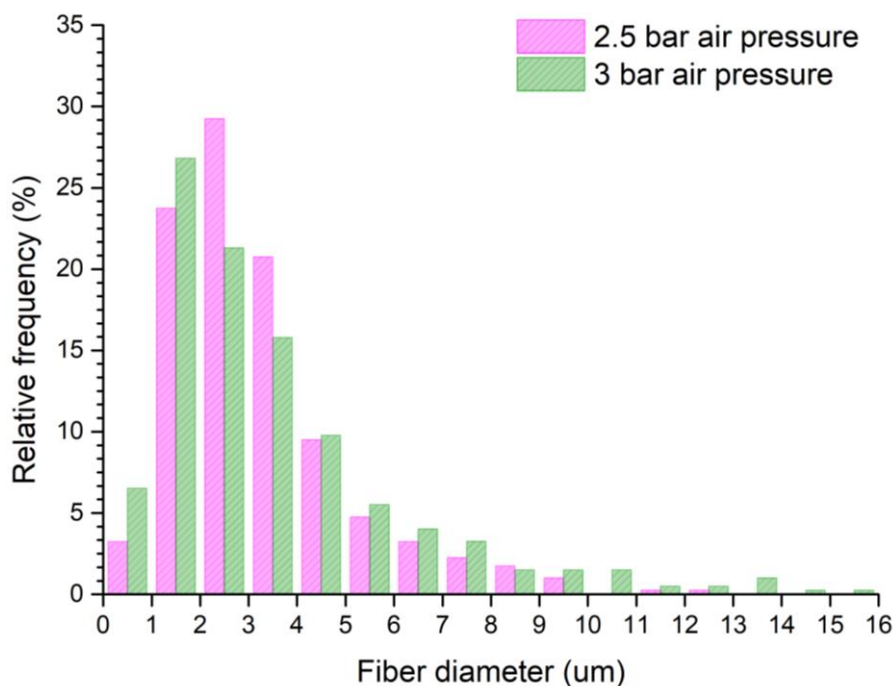
Mean	Standard Deviation	Minimum	Median	Maximum	Mean	Standard Deviation	Minimum	Median	Maximum
3.033	2.094	0.340	2.464	13.830	3.676	2.489	0.454	2.976	15.869

Figure 15: Fiber diameter distribution and respective statistical results for the used solution flow rates of 5 mL/h (left) and 6 mL/h (right).

The solution flow rate of 5 mL/h overall offered fibers with a lowest MFD of 3.03 μm against the 6 mL/h flow rate which had MFD of 3.68 μm . This is probably due to the fact that a lower solution flow rate allows better solvent evaporation and less jet instability resulting in more well defined fiber production. However, it has to be reported that for the flow rate of 5 mL/h clogging of the nozzle occurred a few times giving to understand that, for this system, the optimal solution flow rate is somewhere between 5 and 6 mL/h.

3.6. Air pressure impact on fiber diameter

As mentioned before, a bigger gas pressure allows for a narrower fiber diameter distribution with less variance and consistent morphology. By the results present in the figure 16 such fact it is not observed. The 3 bar air pressure had a bigger MFD followed by a bigger deviation. This might indicate that the 3 bar (~ 45 psi) pressure might be out of the optimal range for fibre production, causing jet instability and preventing solvent from full evaporation (Daristotle et al., 2016; Zhang et al., 2009.).



Mean	Standard Deviation	Minimum	Median	Maximum	Mean	Standard Deviation	Minimum	Median	Maximum
3.215	1.854	0.340	2.658	12.326	3.525	2.653	0.454	2.645	15.869

Figure 16: Fiber diameter distribution for the used air pressures and respective statistical results gathered for the 2.5 bar (bottom left) and 3 bar (bottom right).

To determine the optimal set of air flow and solution flow rate conditions, a few more experiments were made. By keeping the solution flow constant at 5 mL/h, the air pressure was varied to 1, 1.25, 1.5, 1.75, 2 and 2.5 bar. It was already concluded that, for the 5mL/h solution flow some clogging might occur at 2.5 bar indicating that it would be productive if the solution flow was increased or the air pressure was decreased for a bit. The mark of 1.75 bar was determined to be the minimal gas pressure necessary to form a jet with a 5 mL/h solution rate. By According to the literature, a smaller solution flow rate would allow a better solvent evaporation and a bigger air flow a smaller fiber diameter distribution (Daristotle et al., 2016). Logically, it would be productive the increase of the air flow at the limit of the turbulence regime and keeping the lowest possible solution flow rate in a way that no clogging was formed. It was decided to keep the air flow at 2.5 bar and gradually increase the solution flow rate to: 5.25, 5.50, 5.75 and 6 mL/h. The determined optimal solution flow rate was around the value of 5.20 mL/h since this value allowed jet formation without clogging or any other disruptions. Therefore, the optimal determined SBS conditions for the used system (PVP + DES) are stated in the table 3.

Table 3: The best determined parameters conditions for the SBS setup.

PVP concentration	Air pressure	Solution flow rate	Working Distance
18% g/mL	2.5 bar	5.2 mL/h	20 cm

The SBS method has allowed for the fabrication of PVP polymeric membranes impregnated with a DES. In order to ensure DES collection and protection, a 3 layer structure was chosen for the upcoming membranes. The mentioned structure consisted in a sandwich of two protective 18% pure PVP layers with the PVP + DES layer in the middle as is shown in figure 17.

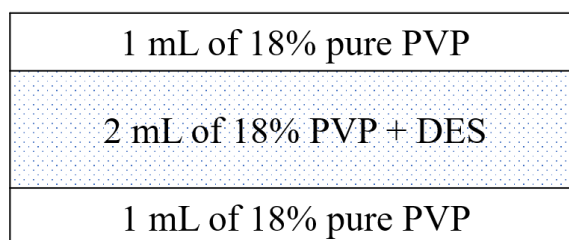


Figure 17: Representation of the final structure of the obtained membranes.

3.7. Drug delivery

In order to evaluate the drug delivery behaviour of the obtained membranes, a PBS (Phosphate Buffered Saline) solution was used as delivery medium in which the membranes were submerged. The liberation profile of the DES containing the ibuprofen was evaluated by UV-Vis Spectroscopy. The ibuprofen has an absorbance peak at around 264 nm and correlation between the absorbance and concentration is according the Beer-Lambert law (1) which states that there is a linear relation between the absorbance and concentration of a substance.

$$Abs = \varepsilon \times l \times C \quad (1)$$

From here, we can build a calibration curve of concentration vs absorbance and create a regression equation that allows the ibuprofen concentration calculation (Sawale, Dhabarde, & Kar Mahapatra, 2016). The obtained calibration curve is available for consulting in the section 6.

Several ways of testing the drug delivery behaviour of the obtained membranes were conducted. At first, a controlled drug delivery assay was made. The membranes were inserted into 20 mL of a 7.4 pH PBS buffer during 24h. Samples of 0.5 mL of the medium were collected at: 5, 10, 15, 30, 45, 60, 120, 180, 240, 300 min and a last one 24h later in order to analyse the drug concentration profile over time. No significative absorbance peaks were detected from the collected samples indicating that the DES was extremely diluted or simply not present in the medium.

The mentioned assay was inconclusive also due to the fact that the membranes were completely dissolved in the medium after 1h to 1h:30. This was due to PVP high solubility in water resulting in full drug liberation in the time the dissolution occurred, being the delivery process mostly dependent of the erosion kinetics of the PVP polymeric chains (Fu & Kao, 2010). Trying to achieve a more controlled drug delivery behaviour, an UV crosslinking of the PVP membranes was made. Polymer crosslinking (in this case by UV light) consists in forming covalent bonds between polymeric chains with the objective of changing some of its physical properties. By crosslinking the PVP membranes, these turned resistant to dissolution, swelling into a hydrogel in the presence of water. In these terms, a hydrogel structure consists of networks that are formed from randomly crosslinked polymeric chains containing a polymeric-network matrix solid phase and an interstitial fluid phase. The hydrogel drug release behaviour is overall slower from the non-crosslinked PVP membranes because it is dependant of more factors like swelling and drug/solvent diffusion rates which are determined by the amount of liquid retained in the hydrogel, the distance between polymer chains and flexibility of those chains (Fu & Kao, 2010; Zarzycki, Modrzejewska, Nawrotek, & Lek, 2010).

3.8. UV Crosslinking and Swelling capacity

Based on the study done by Faria (Faria, 2016), an exposure time of 50 min at 254 nm of wavelength in the irradiation chamber (figure 18) should effectively crosslinked the PVP chains. The UV-crosslinked membranes showed to have very good swelling behaviours both on water and ethanol absorbing the liquids and retaining them for several days without significant dissolution.

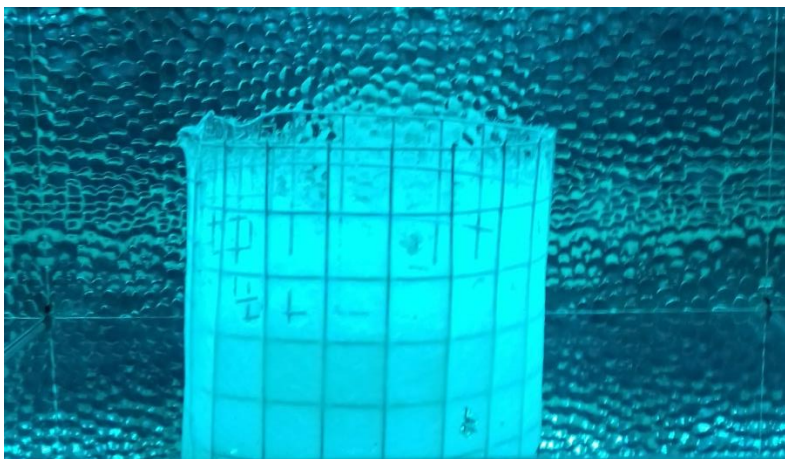


Figure 18: UV crosslinking of polymeric membrane at irradiation chamber.

To test the efficiency of the UV crosslinking, small pieces of one membrane for each DES concentration were cut and submerged on 2 mL of water quickly swelling and forming gels in its presence. Then the samples were placed in the heater during 24h for drying. Such procedure allows to determine the percentage of Sol/Gel mass of each membrane after the UV curing indicating if the used conditions promoted an effective

crosslink of the membranes. The Gel is the fraction of polymeric material that has been successfully crosslinked and managed to swell in the presence of water. As for the Sol fraction, it represents the fraction that was not crosslinked and therefore was flushed by the solvent. The obtained results are present in the following table.

Table 4: Swelling capacity results of tested membranes.

DES Concentration	0	0.5%	1%	2%
% Gel	58.1 ± 1.1	44.6 ± 1.4	65.9 ± 0.7	65 ± 1.2
% Sol	41.9 ± 1.1	55.4 ± 1.4	34.1 ± 0.7	35 ± 1.2

The obtained results show that the used crosslinking procedure was not completely successful and just being effective by around 2/3 of total of the polymeric chains as concluded from the obtained Gel percentages. In order to increase its effectiveness, the exposure time could be increased but Faria reported in his work that, for an exposure time of 60 min, cracks were visible in the fibers surface possibly indicating excessive UV exposure time.

Thermal crosslinking of the membranes was also tried in this work. A PVP membrane was placed in the heater at 150°C (Burnett & Heldreth, 2017) during 1h. After the procedure, the polymeric membrane presented a yellow colour and a strange scent. Such facts indicate that the DES was degraded, and this is not suitable for the purpose of this work. Other crosslinking methods consist in using chemical agents which may compromise the biocompatibility and integrity of our membranes and therefore were not considered.

Although the crosslinking was not fully successful, the membranes did no longer dissolved themselves completely in the PBS. Instead, they quickly swelled in the medium making it denser and cloudy in a way that it was not possible to collect reliable samples to use in the spectrophotometer.

At this point, it was still unclear if the impregnation of the DES within the PVP membranes was being successful using the coaxial SBS method. To ensure that there was DES among the fibrous membranes and to calculate how much of it, a different procedure was made. A single non-crosslinked membrane of each DES concentration was cut in five similar pieces that were individually dissolved at the end of approximately 30 min in 2mL of PBS. At first sight, there were some differences between the five obtained samples, some were cloudier than the others and had a much stronger menthol scent. Since the DES used was not soluble in water, when in contact with the PBS, a cloudy phase appeared. This was confirmed by mixing a few drops of the DES with water observing

the same effect. When these samples were analysed on the spectrophotometer, some of them needed to be diluted in order to fit into the Beer-Lambert law standards due to very high ibuprofen absorbance peaks. The obtained results for this experiment are present in table 5.

Table 5: Results of the delivery of ibuprofen into PBS at room temperature.

DES Concentration (% w/v)	Dissolved membrane mass (mg)	Abs at 264 nm	Dilution Factor	Determined ibuprofen concentration (g/L)	Ibuprofen released mass* (mg)	Theoretical ibuprofen mass** (mg)
0.5	115	-	-	-	2.126	3.056
	102	0.767	1:2	0.764		
	75	-	-	-		
	64	-	-	-		
	50	0.304	1:2	0.299		
1	55	0.781	0	0.389	3.318	6.111
	42	0.576	0	0.286		
	54	0.742	0	0.369		
	50	0.677	0	0.337		
	41	0.56	0	0.278		
2	65	0.75	1:4	1.493	10.743	12.223
	52	0.46	1:4	0.911		
	50	0.519	1:4	1.030		
	44	0.434	1:4	0.859		
	58	0.543	1:4	1.078		

*total mass of ibuprofen experimentally calculated that a whole membrane provided.

**total theoretical ibuprofen mass that a whole membrane could provide.

The previous table shows the results obtained for all samples with well-defined absorbance peaks in the 264 nm region. Knowing the volume of our samples, by using our previous determined calibration curve equation and the Beer-Lambert law, it is possible to determine the amount (mass) of ibuprofen present in the samples. By summing up those values, we can obtain the total of ibuprofen in our entire membrane and compare it with the estimation made for the total possible mass that one membrane can have for each DES concentration. Those values are presented on the 2 rows at the right of the previous listed table and suggest that there are losses during the SBS process. Such fact it is of no surprise at all since the method was not performed in controlled and isolated environment and that there was, indeed, loss of fiber and certainly DES during the process. The fact that the biggest loss comes for the 1% concentration membrane is most likely due to a misalignment between the jet and the collector.

3.9. DES distribution analysis

The fact that, for the concentration of 0.5%, some parts of the membrane had no significant absorbance peaks led to question if the DES distribution through the membrane was being uniform. To analyse this distribution, a total of 15 small pieces from different areas of the membrane were cut to analyse the DES distribution across the membrane. Figure 19 can show how the distribution was evaluated.

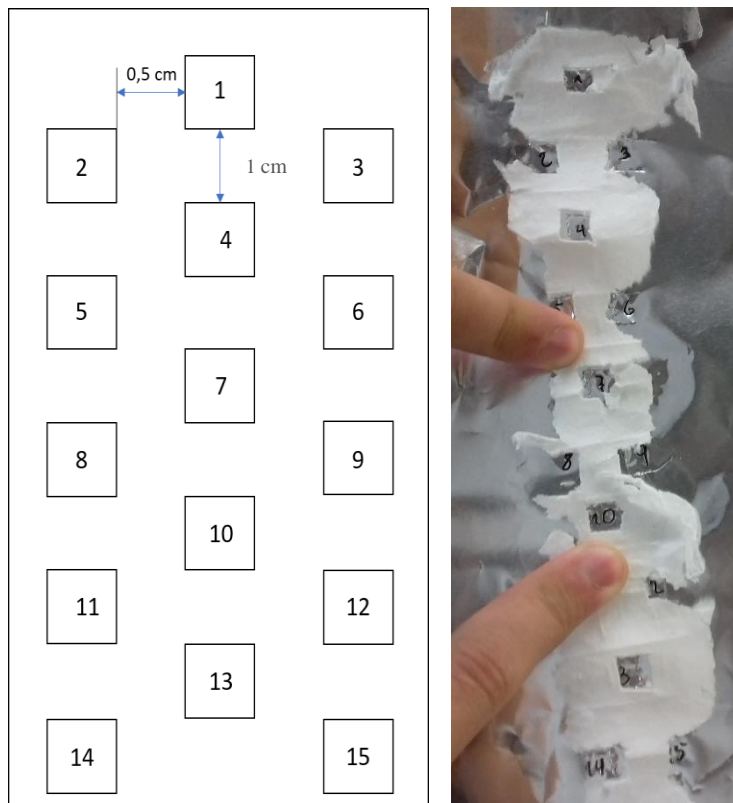


Figure 19: Illustration of the approach taken into analysing DES distribution through the PVP membrane.

The obtained absorbance results for all the samples collected are present in the figure 20.

	DES concentration		
	0.5%	1%	2%
1	-	0.078	0.096
2	0.055	0.050	0.119
3	-	-	0.127
4	0.068	0.092	0.267
5	0.030	-	-
6	-	-	0.393
7	0.101	0.049	0.241
8	0.034	0.029	0.103
9	-	0.029	0.213
10	0.098	0.101	0.226
11	-	0.021	0.228
12	-	0.016	0.274
13	0.150	0.168	0.487
14	0.045	0.114	-
15	0.138	-	-

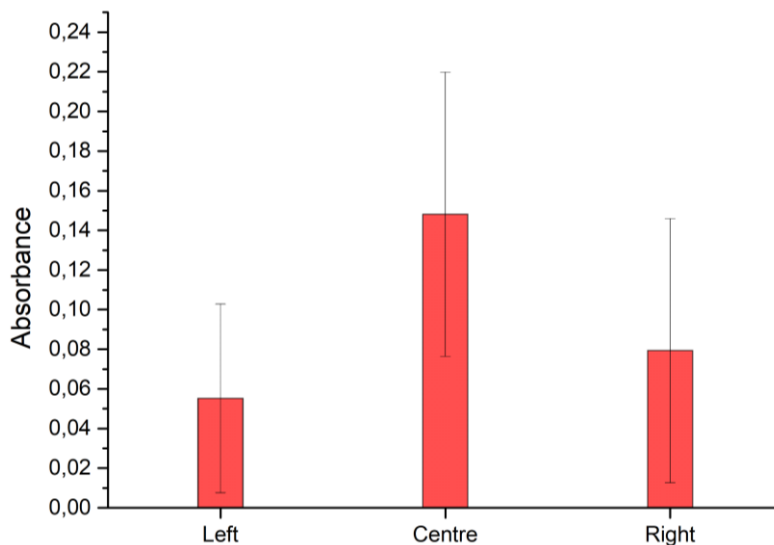


Figure 20: Absorbance values in each site for each DES concentration (left) and average absorbance relation with the zone of the analysed membranes (right).

By observing the data on the figure 20, it is possible to conclude that most of the DES is placed close to the centre of the membrane. On top of that, it is noticeable a slight discrepancy between the left and right-side values, however with no statistical significance. This slight difference must also probably be due to some jet oscillations during the SBS process and a misalignment between the polymer jet and the collector reinforcing the fact that the method needs to be done in a stable environment and conditions. However, as said before, the differences observed have no statistical significance.

3.10. Mechanical tests

To test the mechanical strength of the obtained 18% PVP membranes, Stress/Strain mechanical assays were made in the total of 3 for each membrane. The obtained stress curves are present in figure 21.

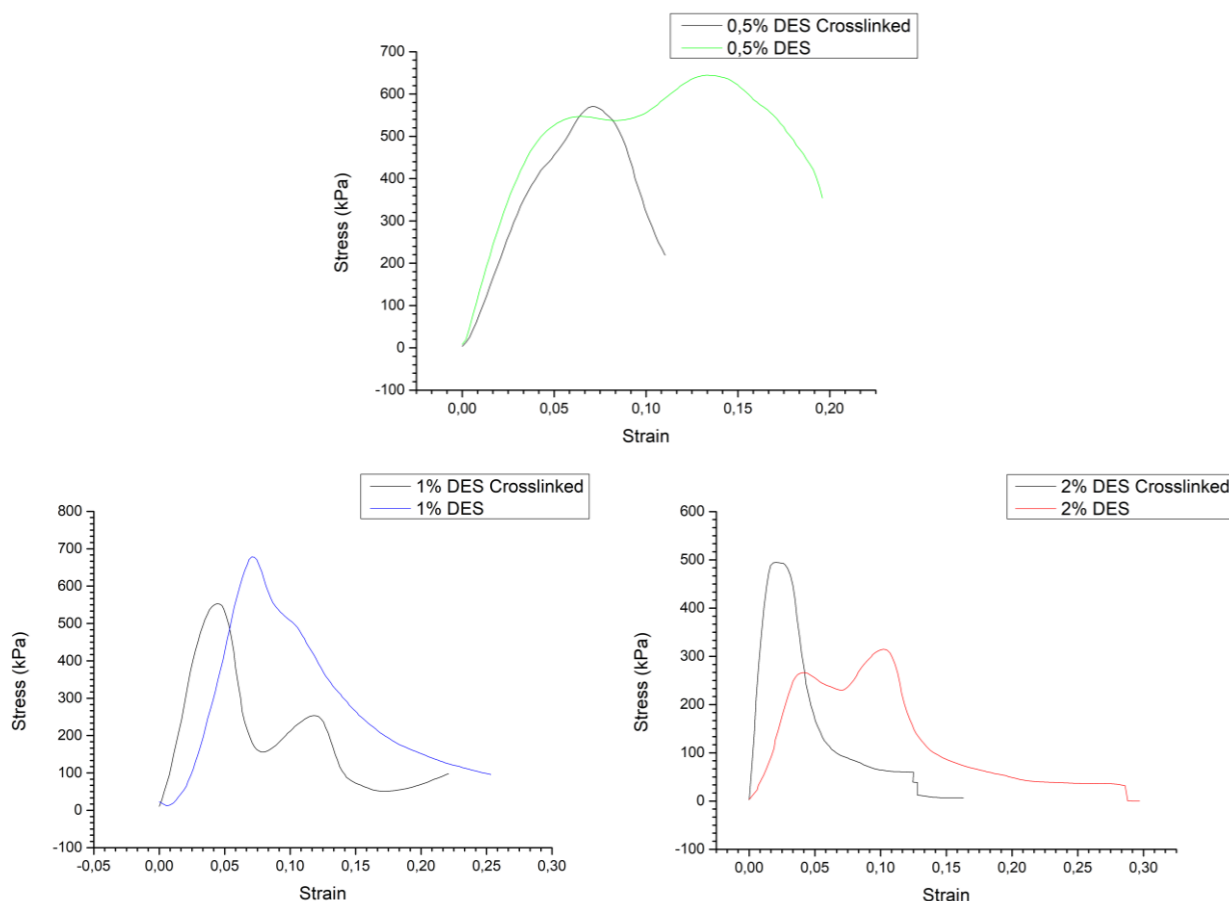


Figure 21: Obtained Stress/Strain graphs for each DES concentration membrane.

From the obtained data, the Young modulus of each membrane was calculated (table 6) and the only objective conclusion gathered is that the membranes that were not submitted to UV curing have a more ductile behaviour than the ones crosslinked. This is no surprise since the crosslinking inhibits the reorganization and reorientation of the molecules according to the shear direction resulting in an increase of brittleness of the membrane (Nielsen, 2008). A ductile behaviour of the membrane is more desirable if the intention is to make an *in situ* deposition since the membrane have a bigger margin to adapt to surrounding forms and to resist to some movements without breaking.

Since fiber deposition is a random process and fiber welding a constant in the process, the mechanical properties of the obtained membranes should present a considerable variance. Such fact is evident and confirmed by the obtained Young modulus values for the 1% and 2% DES crosslinked membranes presented in table 6. Future works should consider the use of more samples to have a meaningful statistical evaluation of the mechanical properties of these membranes.

Table 6: Obtained Young modulus for each membrane.

Sample	Young modulus (E)
0.5 DES	17.0 ± 6.8 MPa
0.5% DES Crosslinked	16.1 ± 4.8 MPa
1% DES	15.3 ± 3.4 MPa
1% DES Crosslinked	27.5 ± 16 MPa
2% DES	13.3 ± 6.7 MPa
2% DES Crosslinked	37.7 ± 23 MPa

Chapter 4 Conclusions and future perspectives

This dissertation reports the optimization of the production of PVP polymeric fibrous membranes impregnated with a menthol:ibuprofen 3:1 DES using the SBS method with the purpose of transdermal delivery of ibuprofen. The SBS method proved to be efficient at fiber fabrication at a faster pace than conventional electrospinning. However, the obtained fibers presented extensive welding as it is commonly observed in fibers produced by this method.

Parameters like polymer concentration, air pressure, solution flow rate were varied and studied in order to obtain the minimum fiber diameter and the most consistent fiber formation in the presence of the eutectic component which came to complicate fiber formation. Regarding polymer concentration, the best concentration for producing pure PVP fibers with the minimum fiber diameter was determined to be placed between 12 and 14% w/v. When the DES was added to the system, it increased solution viscosity causing instability on fiber jet formation at same time that prevented proper solvent evaporation, impairing fiber formation. Because of this, an hair-dryer was added to the SBS assembly in order to slightly increase the surrounding temperature of the jet up to 50°C and polymer concentration was increased to 18% to ensure the lowest mean fiber diameter while ensuring that fiber welding was reduced as much as possible. The polymer concentration proved to be the most important factor in fiber formation using the SBS method and the best SBS setup conditions to produce fibrous membranes from polymeric solutions with 0.5, 1 and 2% w/v DES were a 18% polymer concentration, a 2.5 bar air pressure and a 5.2 mL/h solution flow rate with a working distance of 20 cm to ensure that solvent was properly evaporated. Under these conditions, micrometric fibers with a mean fiber diameter ranging between 1 and 5 μm were obtained. Another feature of the obtained fibers was their helicoidal morphology. Even though the origin of the phenomenon was unknown, fibers with such morphology can be useful for other purposes since the superficial area per volume ratio increases.

The produced polymeric membranes quickly dissolved themselves in water resulting in fast release of the DES into aqueous medium. In order to achieve a slower delivery profile, a UV crosslinking at 254 nm wavelength was performed, crosslinking the membranes up to approximately 60% of their total mass. The UV crosslinking allowed for the membranes to resist dissolution and instead swelling in the presence of water, being able to retain it for long periods of time (more than two weeks). In theory, this can retard drug delivery into the skin. A controlled release of the API was not achieved but if the polymer were deposited directly into the skin, the release rate would be severely

affected and dependent by the degradation ratio of the polymer itself. When PVP makes skin contact, it sticks to it and its easily degraded by it. It is assumed that, at same time the polymeric membrane is being degraded, it will release the DES into the skin (Fu & Kao, 2010). To be certain of this and to understand the ibuprofen delivery profile over time, more tests needed to be done.

When in contact with the skin, according to supporting literature, our DES offers some advantages that come to enhance skin permeation. The already mentioned fact that by being an eutectic, and therefore by having a low melting point, has a higher lipid solubility increasing transdermal permeation. Regarding its chemical composition, menthol has been widely reported as good skin permeation enhancer. It is a low molecular weight molecule that can interact with the lipid structure of the skin disrupting the intercellular lipid structure and opening paths from which the APIs can pass. As for the ibuprofen itself, it is also a low molecular weight molecule with very low lipophilicity, so it penetrates through the skin relatively well. Other studies reinforce that the combination of these two components showed to be much more effective at permeating the skin than when not combined (Alexander et al., 2012; Barry, 1991; Sapra, Jain, & Tiwary, 2008; Stott et al., 1998; Williams & Barry, 2004).

On top of this, mechanical stress/strain studies were performed. The mats did not present a stable mechanical behaviour and the only conclusions were that the membranes had an average Young modulus of 21.2 MPa and that the crosslinked membranes were more brittle than the non-irradiated ones.

A possible way to obtain a lower mean fiber diameter was to use a SBS system in which the interior nozzle, the one through which the polymeric solution flowed, had an inferior diameter than the one used. This because a lower nozzle diameter would allow for lower fiber diameter as literature states. Also, instead of adding an hair-dryer to the montage, a previous warmed up air stream should be more practical. The achieved conclusions of the performed study show great promise for future developments of SBS systems for *in situ* depositions like, wound dressings, burning treatments, surgery coatings among others due to its versatility of use compared to the electrospinning process. For this specific subject, more studies need to be conducted regarding the DES liberation and skin permeation, but its encapsulation and protection was well succeeded giving the so much admired eutectic solvents new hopes of utility.

Chapter 5 References

- Alexander, A., Dwivedi, S., Ajazuddin, Giri, T. K., Saraf, S., Saraf, S., & Tripathi, D. K. (2012). Approaches for breaking the barriers of drug permeation through transdermal drug delivery. *Journal of Controlled Release*, 164(1), 26–40. <https://doi.org/10.1016/j.jconrel.2012.09.017>
- Aroso, I. M., Silva, J. C., Mano, F., Ferreira, A. S. D., Dionísio, M., Sá-Nogueira, I., Duarte, A. R. C. (2016). Dissolution enhancement of active pharmaceutical ingredients by therapeutic deep eutectic systems. *European Journal of Pharmaceutics and Biopharmaceutics*, 98, 57–66. <https://doi.org/10.1016/j.ejpb.2015.11.002>
- Babu, R. J., & Pandit, J. K. (2005). Effect of penetration enhancers on the transdermal delivery of bupranolol through rat skin. *Drug Delivery: Journal of Delivery and Targeting of Therapeutic Agents*, 12(3), 165–169. <https://doi.org/10.1080/10717540590931936>
- Barry, B. W. (1991). Modern methods of promoting drug absorption through the skin. *Molecular Aspects of Medicine*, 12(3), 195–241. [https://doi.org/10.1016/0098-2997\(91\)90002-4](https://doi.org/10.1016/0098-2997(91)90002-4)
- Benson, H. A. (2005). Transdermal drug delivery: penetration enhancement techniques. *Curr Drug Deliv*, 2(1), 23–33. <https://doi.org/10.2174/1567201052772915>
- Burnett, C. L., & Heldreth, B. (2017). PVP (Polyvinylpyrrolidone). *International Journal of Toxicology*, 36(5_suppl2), 50S–51S. <https://doi.org/10.1177/1091581817716649>
- Chhabra, R. P. (2010). Non-Newtonian Fluids: An Introduction BT - Rheology of Complex Fluids. In J. M. Krishnan, A. P. Deshpande, & P. B. S. Kumar (Eds.) (pp. 3–34). New York, NY: Springer New York. https://doi.org/10.1007/978-1-4419-6494-6_1
- Daristotle, J. L., Behrens, A. M., Sandler, A. D., & Kofinas, P. (2016). A Review of the Fundamental Principles and Applications of Solution Blow Spinning. *ACS Applied Materials and Interfaces*, 8(51), 34951–34963. <https://doi.org/10.1021/acsami.6b12994>
- Fu, Y., & Kao, W. J. (2010). Drug release kinetics and transport mechanisms of non-degradable and degradable polymeric delivery systems. *Expert Opinion on Drug Delivery*, 7(4), 429–444. <https://doi.org/10.1517/17425241003602259>
- Greenhalgh, R. D., Ambler, W. S., Quinn, S. J., Medeiros, E. S., Anderson, M., Gore, B., Blaker, J. J. (2017). Hybrid sol–gel inorganic/gelatin porous fibres via solution blow spinning. *Journal of Materials Science*, 52(15), 9066–9081. <https://doi.org/10.1007/s10853-017-0868-1>
- Haaf, F., Sanner, A., & Straub, F. (1985). Polymers of N-Vinylpyrrolidone: Synthesis, Characterization and Uses. *Polymer Journal*, 17, 143. Retrieved from <http://dx.doi.org/10.1295/polymj.17.143>
- Hadgraft, J. (1979). The epidermal reservoir; A theoretical approach. *International Journal of Pharmaceutics*, 2(5–6), 265–274. [https://doi.org/10.1016/0378-5173\(79\)90033-4](https://doi.org/10.1016/0378-5173(79)90033-4)

- Huang, Z. M., Zhang, Y. Z., Kotaki, M., & Ramakrishna, S. (2003). A review on polymer nanofibers by electrospinning and their applications in nanocomposites. *Composites Science and Technology*, *63*(15), 2223–2253. [https://doi.org/10.1016/S0266-3538\(03\)00178-7](https://doi.org/10.1016/S0266-3538(03)00178-7)
- Kalluri, H., & Banga, A. K. (2011). Formation and closure of microchannels in skin following microporation. *Pharmaceutical Research*, *28*(1), 82–94. <https://doi.org/10.1007/s11095-010-0122-x>
- Kunta, J. R., Goskonda, V. R., Brotherton, H. O., Khan, M. A., & Reddy, I. K. (1997). Effect of menthol and related terpenes on the percutaneous absorption of propranolol across excised hairless mouse skin. *Journal of Pharmaceutical Sciences*, *86*(12), 1369–1373. <https://doi.org/10.1021/js970161+>
- Liechty, W. B., Kryscio, D. R., Slaughter, B. V., & Peppas, N. A. (2010). Polymers for Drug Delivery Systems. *Annual Review of Chemical and Biomolecular Engineering*, *1*(1), 149–173. <https://doi.org/10.1146/annurev-chembioeng-073009-100847>
- Liu, X., Xu, Y., Wu, Z., & Chen, H. (2013). Poly(N-vinylpyrrolidone)-Modified surfaces for biomedical applications. *Macromolecular Bioscience*, *13*(2), 147–154. <https://doi.org/10.1002/mabi.201200269>
- Medeiros, E. S., Glenn, G. M., Klamczynski, A. P., Orts, W. J., & Mattoso, L. H. C. (2009). Solution blow spinning: A new method to produce micro- and nanofibers from polymer solutions. *Journal of Applied Polymer Science*, *113*(4), 2322–2330. <https://doi.org/10.1002/app.30275>
- Faria, J. (2016). Production and optimization of hybrid fibrillary gels by colloidal electrospinning.
- Nielsen, L. E. (2008). Journal of Macromolecular Science , Part C : Polymer Reviews Cross-Linking – Effect on Physical Properties of Polymers. *Journal of Macromolecular Science, Part C: Polymer Reviews*, *3*(1), 69–103. <https://doi.org/10.1080/15583726908545897>
- Ramakrishna, S., Fujihara, K., Teo, W.-E., Lim, T.-C., & Ma, Z. (2005). *An Introduction to Electrospinning and Nanofibers*. WORLD SCIENTIFIC. <https://doi.org/doi:10.1142/5894>
- Rowe, R., Sheskey, P., & Quinn, M. (2009). Handbook of Pharmaceutical Excipients. *Handbook of Pharmaceutical Excipients, Sixth Edition*, 549–553. [https://doi.org/10.1016/S0168-3659\(01\)00243-7](https://doi.org/10.1016/S0168-3659(01)00243-7)
- Santos, A. M. C., Medeiros, E. L. G., Blaker, J. J., & Medeiros, E. S. (2016). Aqueous solution blow spinning of poly(vinyl alcohol) micro- and nanofibers. *Materials Letters*, *176*, 122–126. <https://doi.org/10.1016/j.matlet.2016.04.101>
- Sapra, B., Jain, S., & Tiwary, A. K. (2008). Percutaneous Permeation Enhancement by Terpenes: Mechanistic View. *The AAPS Journal*, *10*(1), 120–132. <https://doi.org/10.1208/s12248-008-9012-0>
- Sawale, V., Dhabarde, D., & Kar Mahapatra, D. (2016). Development and Validation of UV Spectrophotometric Method for Simultaneous Estimation of Olmesartan Medoxomil and Chlorthalidone in Bulk and Tablet. *Eurasian Journal of Analytical Chemistry*, *12*(1), 55–66. <https://doi.org/10.12973/ejac.2017.00144a>

- Smith, L. E., Rimmer, S., & MacNeil, S. (2006). Examination of the effects of poly(N-vinylpyrrolidone) hydrogels in direct and indirect contact with cells. *Biomaterials*, 27(14), 2806–2812. <https://doi.org/10.1016/j.biomaterials.2005.12.018>
- Stott, P. W., Williams, A. C., & Barry, B. W. (1998). Transdermal delivery from eutectic systems: Enhanced permeation of a model drug, ibuprofen. *Journal of Controlled Release*, 50(1–3), 297–308. [https://doi.org/10.1016/S0168-3659\(97\)00153-3](https://doi.org/10.1016/S0168-3659(97)00153-3)
- Teodorescu, M., & Bercea, M. (2015). Poly(vinylpyrrolidone) – A Versatile Polymer for Biomedical and Beyond Medical Applications. *Polymer - Plastics Technology and Engineering*, 54(9), 923–943. <https://doi.org/10.1080/03602559.2014.979506>
- Ulbrich, K., Holá, K., Šubr, V., Bakandritsos, A., Tuček, J., & Zbořil, R. (2016). Targeted Drug Delivery with Polymers and Magnetic Nanoparticles: Covalent and Noncovalent Approaches, Release Control, and Clinical Studies. *Chemical Reviews*, 116(9), 5338–5431. <https://doi.org/10.1021/acs.chemrev.5b00589>
- Williams, A. C., & Barry, B. W. (2004). Penetration enhancers. *Advanced Drug Delivery Reviews*, 56(5), 603–618. <https://doi.org/10.1016/j.addr.2003.10.025>
- Yu, T. (2017). Surfactant Assisted Dispersion of Single-Walled Carbon Nanotubes in Polyvinylpyrrolidone Solutions. *Colloid and Surface Science*, 2(3), 96–106. <https://doi.org/10.11648/j.css.20170203.12>
- Zarzycki, R., Modrzejewska, Z., Nawrotek, K., & Lek, U. (2010). Drug Release From Hydrogel Matrices. *Ecological Chemistry and Engineering S*, 17(2), 117–136.
- Zhang, L., Kopperstad, P., West, M., Hedin, N., & Fong, H. (n.d.). Generation of polymer ultrafine fibers through solution (air-) blowing. *Journal of Applied Polymer Science*, 114(6), 3479–3486. <https://doi.org/10.1002/app.30938>

Chapter 6 Attachments

6.1. Polymeric solutions preparation

The following tables comes to present some of the quantities measured in the preparation of 5 mL of the polymeric solutions used in membranes fabrication.

Table 7: Some experimental values of the measured mass of PVP for 18% PVP concentration.

	Theoretical value (g)	Experimental value (g)
1	0.9000	0.9045
2		0.9127
3		0.9023
4		0.9171
5		0.9183

Table 8: Some experimental values of the measured mass of DES for 0.5% DES concentration.

	Theoretical value (g)	Experimental value (g)
1	0.0250	0.0312
2		0.0424
3		0.0295
4		0.0337
5		0.0361

Table 9: Some experimental values of the measured mass of DES for 1% DES concentration.

	Theoretical value (g)	Experimental value (g)
1	0.0500	0.0628
2		0.0612
3		0.0573
4		0.0569
5		0.0635

Table 10: Some experimental values of the measured mass of DES for 2% DES concentration.

	Theoretical value (g)	Experimental value (g)
1	0.1000	0.1231
2		0.1201
3		0.1045
4		0.1172
5		0.1153

Table 11: Some experimental values of the measured mass of PVP for 20% PVP concentration.

	Theoretical value (g)	Experimental value (g)
1	1.0000g	1.0343
2		1.0012
3		1.1592
4		1.2837
5		1.1726

6.2. MFD values resulting from SBS optimization study

Table 12: MFD for all variations done during the SBS process.

Essay	C PVP (g/mL %)	C DES (g/mL%)	Q sol (mL/h)	Air Pressure (bar)	MFD (μm)
1	18%	0%	5	3	5.63
2				2.5	1.77
3			6	3	2.76
4				2.5	5.03
5		0.5%	5	3	5.12
6				2.5	2.82
7			6	3	3.19
8				2.5	1.73
9		1%	5	3	1.69
10				2.5	2.08
11			6	3	1.91
12				2.5	3.05
13		2%	5	3	2.14
14				2.5	2.80
15			6	3	1.79
16				2.5	2.73
17	20%	0%	5	3	1.64
18				2.5	1.84
19			6	3	1.85
20				2.5	3.36
21		0.5%	5	3	1.99
22				2.5	3.00
23			6	3	4.04
24				2.5	3.34
25		1%	5	3	3.02
26				2.5	2.9
27			6	3	5.47
28				2.5	3.68
29		2%	5	3	2.50
30				2.5	4.64
31			6	3	3.85
32				2.5	2.87

6.3. Ibuprofen calibration curve

The obtained calibration curve for ibuprofen in water is presented on figure 22 and the curve parameters are stated in table 7.

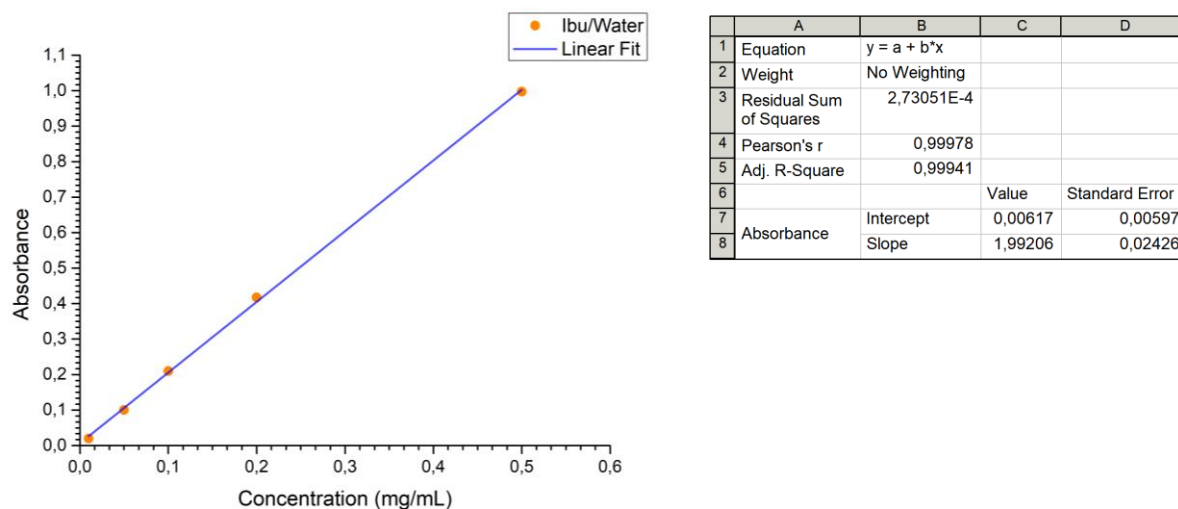


Figure 22: Obtained calibration curve for ibuprofen release in aqueous medium.

Table 13: Ibuprofen calibration curve parameters.

Parameters	Ibuprofen
Detection wavelength	264 nm
Linearity range	0.01-0.5 mg/mL
Slope (a)	1.99206
Intercept (b)	0.00617
Correlation coefficient	0.99941
Regression equation ($y=ax+b$)	$y=1.99206x+0.00617$

6.4. PBS solution recipe

The respective components needed and measured to produce 1L of PBS solution, are presented in the following table.

Table 14: PBS recipe components.

Component	Theoretical mass value (g)	Measured mass value (g)
NaCl	8	8.0076
KCl	0.2	0.2077
Na ₂ HPO ₄	1.44	1.4402
KH ₂ PO ₄	0.24	0.2464

After its measure, each component was added to 1L of distilled water and placed in magnetic stirring for 1h. After that, the pH was adjusted to approximately 7.4 by adding a few drops of NaOH.

6.5. DES molecular weight and density

Ibuprofen (C₁₃H₁₈O₂) Mw = 206.285 g/mol

Menthol (C₁₀H₂₀O) Mw = 156.269 g/mol

DES 3:1 Menthol:Ibuprofen Mw = 675.092 g/mol

Five samples of 0.5 mL of DES were collected and weighted. The obtained results are present in table

Table 15: Mass values of each sample measured.

	DES weight (mg)
1	333
2	429
3	414
4	433
5	678

DES density $\approx 457.4 \pm 221$ g/L